

Mohamed KhiderUniversity of Biskra

Faculty of exact sciences Material sciences department

MASTER MEMORY

Matter Sciences Section of Physics Specialty of Matter Physics

Réf.:

Presented by: Dalel ZOUAOUI THE:

Preparation and Characterizations of F Doped NiS Thin Films by Deposition Spray Method

Jury:

Mr.	Said LAKEL	Professor	University of Biskra	Presidant
Mr.	Said BENRAMACHE	Professor	University of Biskra	Supervisor
Mrs	Zahia BENCHAREF	MCA	University of Biskra	Examiner

Academic Year: 2024-2025

إهداء

المن علّمني القوة في ضعفي، والثبات في محني، الله من كان سندي في الحياة، ولم يفارقني بالدعاء حتى بعد رحيله، الهي روح أبي الطاهرة "زواوي عمار"، رحمة الله عليه، أهدي ثمرة جهدي، ودعائي أن يجعل الله هذا العمل في ميزان حسناته.

والمن نبع الحنان، وعين الرضا، إلى أمي الغالية "لبعل مليكة"، التي كانت وما زالت مصدر دعمي الأول، لكِ كل الامتنان، وكل الحب، وكل ما في القلب من شكر.

والمن المخوتي الأعزاء، "توفيق، حمزة، لويزة، عادل، عامر، هاني، رانية و داود"من شاركوا خطواتي، وكانوا عوني في مسيرتي، أنتم فخري وسندي. والمن حففن والمن والمناه وكالمناه والمناه والمناه

Dedication

To the one who taught me strength in my weakness, and steadfastness in my trials, to the one who was my support in life, and who never ceased to pray for me even after his departure, to the pure soul of my father "Zouaoui Ammar", may God have mercy on him, I dedicate the fruit of my efforts, and pray that God places this work in the balance of his good deeds.

And to the source of tenderness and the eye of contentment, to my dear mother "Lbaal Malika", who was and still is my primary source of support, to you, all my gratitude, all my love, and all the thanks in my heart.

And to my dear siblings, "Toufik, Hamza, Louiza, Adel,
Amer, Hani,Rania, Daoud", who shared my steps and were
my support on my journey, you are my pride and my support.
And to my dear friends, "Ilham, Marwa, Suheila, Salima",
my companions on this journey, who have eased my burdens
along the way, thank you for every moment of support and
every sincere word.

Acknowledgement

Praise be to God, by whose grace good deeds are completed, and by whose guidance difficulties are overcome and achievements are realized.

So to Him, the Most High, I raise my hands in gratitude and praise, for He has blessed me with strength, patience, and determination until I completed this work, hoping that it will be in the balance of my good deeds and benefit me and others.

I must also mention the personal effort I put in, and the perseverance and continuous striving I achieved throughout the stages of this research, despite the challenges and difficulties, believing in the value of knowledge and the nobility of its goals.

I extend my heartfelt thanks and appreciation to **Professor Said BENRAMACHE** for his support and scientific follow-up, and for his profound observations that enriched this work and contributed to guiding it towards improvement. He has my utmost gratitude and appreciation.

I would like to extend my special thanks to Professor and **Dr. Amira SBAIHI** for her valuable guidance, continuous encouragement, and clear commitment to the quality and precision of scientific work. May God reward her generously and bless her knowledge and contributions.

I do not forget

Thanks to the members of the esteemed scientific committee to discuss my thesis, **Pr. Said LAKEL** at university of biskra as the chair of the committee, and **Dr. Zahia BENCHAREF** at university of biskra as a discussant, I hope you like this work and I am open to your criticism.

TABLE OF CONTENTS

الإهداء	i
Dedecation	ii
Acknowledgement	iii
Table of Contents	iv
Abstract	vi
الملخص	vi
Liste of Tables	vii
Liste of figures	viii
General Introduction	1
Chapter one: Thin Films and their applications	4
I.1. Introduction	5
I.2. Thin films	5
I.3. Semiconductor Materials	6
I. 4. Presentation of Nickel sulfide	7
I. 4. 1. Structural Properties	8
I. 4 .2. Optical Properties	10
I. 4. 3. Electrical properties	11
I. 5. Nickel sulfide applications	12
I. 5. 1. Electrodes of LIBs and Supercapacitors (SCs)	12
I. 5. 2. Oxygen Reduction Reaction (ORR)	13
I. 6. Semiconductors Doping	13
I. 7. Thin Film Deposition Methods	14
I. 7.1. Pulsed Laser Deposition (PLD)	15
I. 7.2. Sputtering	15
I. 7.3. Thermal Evaporation	16
I. 7.4. Chemical VaporDeposition (CVD)	16
I. 7.5. Spin Coating	16
I. 7.6. Spray deposition method	16
I. 8.Fluoride	17
I. 8. 1. Definition	17
I. 8. 2. The physical properties of fluoride	17
I. 9. Conclusions	18
References	18

Chapter two: Experimental parts	21
II.1. Introduction	22
II.2. Generalities on spray pyrolysis technique (SPT)	22
II.2.1 Advantages of spray pyrolysis Technique	22
II.2.2 Disadvantages of spray pyrolysis Technique	23
II.2.3 Classification & equipment of Spray Pyrolysis Technique	23
II.3. Principle of deposition processes in spray pyrolysis	24
II.3.1. Atomization of the precursor solution	24
II.3.2. Aerosol transport of the droplet	25
II.3.3. Decomposition of the precursor to initiate film growth	25
II.4. Protocol methodology	25
II.4.1 Preparation of spray solution	25
II.4.2 Preparation of the Films	26
II. 5. Charactirization techniques	28
II. 5. 1. X-Ray diffraction technique (XRD)	28
II. 5. 1. 1.The Lattice parameters	28
II. 5. 1. 2.The Crystallites size (D)	29
II. 5. 1. 3.The dislocations density	30
II. 5.2. Spectroscopy UV-VISIBLE	30
II. 5. 3. Four-probe method	32
II.5.3. Fourier Transform Infrared Spectroscopy (FTIR)	33
II. 7. Conclusion	34
References	34
Chapter there: Results and Discussions	37
III.1. Introduction	38
III.2. Experimental procedure	38
III.3. Structural properties	39
III.4. FTIR Spectroscopy results	43
III.5. AFM analysis	44
III.5. Electrical properties	45
III.7. Conclusions	47
References	48
General Conclusion	50

Abstract

In this work, the F doped NiS thin films were successfully deposited on glass substrate by spray pneumatic method. F doped NiS solutions were prepared by dissolving (0.15 M) an amount of nickel nitrate hexahydrate (Ni(NO₃)₂.6H₂O) and thiourea (CS(NH₂)₂) as a source of nickel Ni and sulfur S respectively, and ammonium fluoride (NHF₄) with the ratio of F/S = 0.01 to 0.05. The effect of F doping on structural, optical, morphologically and electrical properties were investigated. The prepared F doped NiS thin films have a polycrystalline nature with a hexagonal structure, the (012) diffraction peak is the preferred orientation. The FTIR analysis showed the characteristic vibration bands of NiS. The AFM analysis revealed that nanometer sized spherical grains cover the entire surface of the films prepared. The minimum sheet resistance was found for the thin film prepared with 1 at% F

Key words: F; NiS; Thin films; Doping Levels; Spray pneumatic.

الملخص

في هذا العمل، تم ترسيب الأغشية الرقيقة من NiS المطعمة بالفلور بنجاح على ركيزة زجاجية بطريقة الرش الهوائي. تم تحضير محاليل NiS المخدرة بالفلور عن طريق إذابة (0.15 مول) من سداسي هيدرات نترات النيكل (Ni(NO₃)₂.6H₂O) كمصدر النيكل، والثيويوريا (CS(NH₂)₂) كمصدر الكبريت، وفلوريد الأمونيوم (NHF₄) بنسبة F/S من 0 إلى 5%. تم التحقيق في تأثير التطعيم بالفلور على الخصائص البنيوية والبصرية والمورفولوجية والكهربائية. تتميز أغشية الرقيقة من NiS المطعمة بالفلور والمحضرة بطبيعة متعددة البلورات ذات بنية سداسية، وتُعد ذروة الحيود (012) هي الاتجاه المفضل. أظهر تحليل FTIR نطاقات الاهتزاز المميزة لـNiS . كما كشف تحليل AFM أن الحبيبات الكروية بحجم النانومتر تغطي السطح بالكامل للأغشية المحضرة. و كما تم العثور على الحد الأدنى لمقاومة الصفائح للفيلم الرقيق المحضر بنسبة F1 %

الكلمات المفتاحية: NiS :F؛ الأغشية الرقيقة؛ مستويات المنشطات؛ الرش الهوائي.

LIST OF TABLES

N ^o						
Chap	Chapter one: Thin Films and their applications					
Table I.1	Compound semiconductor materials listed by group and in order of increasing band-gap energy ranging from the near-IR to XUV wavelengths.	7				
Table I. 2	The preferred orientation, Structure and Crystallite size of various deposited NiS thin films.	9				
Table I.3	The transmittance /absorbance and the optical band gap (Eg) of various deposited NiS thin films.	11				
Table I.4 The physical properties of fluoride						
	Chapter there: Results and Discussions					
Table III.1	The crystal structure corresponding to each <hkl> plane.</hkl>	41				
Table III.2	The the diffraction angle corresponding to each <hkl>plane.</hkl>	42				
Table III.3	The Crystallite size values for each <hkl>plane of FxNiS1-x films.</hkl>	42				
Table III.4	The Micro-Strain values for each <hkl>plane of FxNiS1-x films.</hkl>	42				
Table III.5	The electrical resistance Cu and F co-doped ZnO thin films	46				

LIST OF FIGURES

N° Pa						
Chap	Chapter one: Thin Films and their applications					
Figure I.1	Depicts the crystal structures of different polymorphic forms of nickel sulfides.					
Figure I.2	Categorization of thin film depositionmethods	15				
	Chapter two: Experimental parts					
Figure II.1	Diagrammatic representation of spray pyrolysis equipment.	23				
Figure II.2	Description of the deposition processes	24				
Figure II.3	Description of the Preparation of the spray solution dopedwithF	26				
Figure II.4	CAT.NO.7101 microscope glass slide	26				
Figure II.5	Preparation of glass substrates	27				
Figure II.6	Description of the Preparation of thin films by (SPT)	27				
Figure II.7	Schematic of X-ray diffraction					
Figure II.8	Diagram of the hexagonal structure of NiS					
Figure II.9	The principal operation of UV-Visible spectrophotometer					
Figure II.10	Schematic of four point method	33				
Figure II.11	Schematic diagram of FTIR Spectrophotometer	34				
	Chapter there: Results and Discussions					
Figure III.1	X-Ray diffraction spectra of F doped NiS thin films	39				
	elaborated at 270°C with various F doping ratio (at.%). The inset graph shows diffraction angle and intensity peaks of					
	the ICSD card No. 98-060-2488.					
Figure III.2	re III.2 a): X-Ray diffraction spectra of F doped NiS thin films at					
	various F doping ratios (at.%) and b): The shifting of specified angle of (012) peak.					
Figure III.3	a): Variaation of crystallite size b): Variation of microstrain values of F doped NiS thin film.	42				
Figure III.4	FTIR spectra of F doped NiS thin film prepared with various fluoride doping.	44				

Figure III.5	AFM micrographs of F doped NiS thin film prepared with various fluoride doping.	
Figure III.6	The variation of voltage and sheet resistance as a function of current with different F doping of NiS thin films.	46
Figure III.7	The variation of sheet resistance as a function of current with different F doping of NiS thin films.	47

General Introduction

General Introduction

Sulfides (TMSs) have become a growing focus of advanced electrode materials in electrochemical supercapacitors. These consist of strong redox activity, distinct crystalline structures, low electro negativity, high electrical conductivity, and large specific capacity. These characteristics have caused recent research to concentrate on nickel sulfide (NiS) electrode materials, mainly for supercapacitor applications. Its rich chemical makeup, high specific capacity, superior electrochemical activity, and environmental friendliness are the reasons for this interest. NiS-based materials are therefore attractive options for supercapacitors because of these characteristics [1-3].

The inorganic compound nickel sulfide (NiS) is a member of the metal sulfide family and is distinguished by its many phases, each of which has its own crystal structure and set of characteristics. A rare mineral called millerite, which is distinguished by its needle-like crystal form, is created by a number of chemical processes, such as the reaction of nickel salts with hydrogen sulfide (H_2S) and high-temperature reactions between nickel and sulfur. Nickel sulfide is found in some types of meteorites in nature. There are two polymorphic forms of this compound: the beta (β) phase, which has a rhombohedral cell at lower temperatures, and the alpha (α) phase, which has a hexagonal unit cell and is stable at high temperatures. NiS structures, like hierarchical microflowers made of layered nanoplates, have been shown in studies to exhibit superior electrochemical stability and high specific capacitance. These developments suggest that NiS has a great deal of promise for creating high-performance supercapacitors [3-6].

In this study, we will explore the characterizations of F doped NiS thin films by spray deposition method. We have prepared an alloy of F doped NiS at various F doping concentrations for study the effect of F doping on structural, optical, morphologically and electrical properties. These films are applied using a single technique: spray pyrolysis. This method offers several benefits, including straightforward and inexpensive equipment, high efficiency in choosing deposition parameters, a wide range of precursor materials, and the ability to operate in an ambient atmosphere. Additionally, it facilitates easy control over the morphology of thin film, ranging from dense to porous, or even fractal types. In this memory, we will study three chapters, each of which is briefly presented below:

The first chapter offers a comprehensive overview, which is represented in applications and properties of nickel sulfide.

General Introduction

The second chapter describes the preparation methods of spray deposition and our experience in preparing the solution as well characterization techniques used in synthesizing of F doped NiS thin films

The third chapter discusses our results and the synthesis of F doped NiS thin films using the spray pyrolysis deposition technique.

Finally, a summary of the chapters is provided, outlining the results of this research work and suggesting avenues for future research.

References

- [1] Yan X, Tong X, Ma L, Tian Y, Cai Y, Gong C, et al. Synthesis of porous NiS nanoflake arrays by ion exchange reaction from NiO and their high performance supercapacitor properties. Mater Lett 2014;124:133–6.
- [2] Zhang H, Yu X, Guo D, Qu B, Zhang M, Li Q, et al. Synthesis of bacteria promoted reduced graphene oxide-nickel sulfide networks for advanced supercapacitors. ACS Appl Mater Interfaces 2013;5:7335–40.
- [3] Guan Y, Hu K, Su N, Zhang G, Han Y, An M. Review of NiS-Based Electrode Nanomaterials for Supercapacitors. Nanomaterials 2023;13:1–35.
- [4] Qu Y, Yang M, Chai J, Tang Z, Shao M, Kwok CT, et al. Facile Synthesis of VanadiumDoped Ni3S2 Nanowire Arrays as Active Electrocatalyst for Hydrogen Evolution Reaction. ACS Appl Mater Interfaces 2017;9:5959–67.
- [5] Kajbafvala M, Moradlou O, Moshfegh AZ. CVD growth of the nanostructured Ni3S2 thin films as efficient electrocatalyst for hydrogen evolution reaction. Vacuum 2021;188:110209.
- [6] Qin JF, Yang M, Hou S, Dong B, Chen TS, Ma X, et al. Copper and cobalt co-doped Ni3S2 grown on nickel foam for highly efficient oxygen evolution reaction. Appl Surf Sci 2020;502:144172.

Chapter one:

Thin Films and their applications

I.1. Introduction

Significant advances in semiconductor physics have resulted in significant study on transparent thin films of metal oxides for optical and electrical applications. These films usually have a broad bandgap (>3 eV) and great transparency, with refractive index and conductivity varying according to the metal oxide type. Common uses include optical coatings such as Al₂O₃ and TiO₂ [1].

The remarkable electronic, optical, and photoelectric properties of transition metal sulfides, such as copper sulfide (CuS), molybdenum sulfide (MoS), nickel sulfide (NiS), and cobalt sulfide (CoS), are well-known. Numerous cutting-edge scientific and technological domains make extensive use of these materials. Because of its distinct phase transition from an antiferromagnetic semiconductor at low temperatures to a paramagnetic metal at high temperatures, nickel sulfide (NiS) stands out among this large group [2].

I. 2. Thin films

Thin films are described as materials generated by random nucleation and growth processes in which atomic, ionic, or molecular species condense and react on a solid support called a substrate [3]. These films come in a variety of thicknesses, from a few nanometers to micrometers. Thin films have unique characteristics that differ greatly from the bulk materials from which they are formed. As the film thins, surface qualities become more important than bulk characteristics.

One of the primary benefits of thin films is their ability to miniaturize components, making them vital for electrical devices. The structural, chemical, metallurgical, and physical characteristics of these materials are largely dependent on the deposition parameters, thickness, crystalline orientation, and deposition processes [3]. Random atomic nucleation and growth introduce novel and unique features into thin film materials [4]. These characteristics may be carefully regulated and replicated by fine-tuning a variety of deposition parameters [3-5].

A thin film is a two-dimensional material layer that is placed on a substrate to attain qualities that are difficult or impossible to achieve in bulk form. A thin film's special feature stems from its unique manufacturing process, which involves the incremental addition of atoms or molecules. Thickness is a key feature of thin films, and it is intimately related to other properties that scale differently with thickness. Thus, thin films are defined by more

than just their thickness. Depending on their thickness, thin films can be utilized in a variety of applications, including magnetic multilayers, optical coatings, tribological coatings, quantum well structures based on super lattices, nanoscale coatings, etc [2-5].

I.3. Semiconductor Materials

In general, semiconductor materials fall into one of two groups. Compound semiconductors, the most prevalent of which are produced from groups III and V (e.g. GaAs, InP) and II and VI (e.g. CdTe) of the periodic table, and elemental semiconductors, Si and Ge, which are generated from elements in group IV of the periodic chart. Compound semiconductors are extremely helpful because to the wide variety of chemicals that are available. Table 1, which lists the semiconductors available as a function of group and bandgap energy, serves as an example of this. Most compounds are soluble in one another in addition to binary materials like GaAs or InP, which enables the synthesis of ternary (like AlGaAs, HgCdTe), quaternary (like InGaAsP, InGaAlP), and higher-order solution, only through the alloying of binary chemicals. Growing chemically pure and structurally flawless crystals with precise stoichiometry is the fundamental challenge in creating detector-grade material. Due to their extensive range of stopping powers and band gaps, compound semiconductors provide several unique benefits over their elemental counterparts for radiation detection. For instance, typical atomic numbers range from 30 to 90 and band-gap energies from 1.35 to 2.6 eV (see TableI.1). In turn, this indicates that materials can be targeted for certain radiation detection applications by mixing and matching available band gaps and stopping powers. As an illustration, it is within a specified goal spectral resolution and detection efficiency [6].

All II-VI semiconductors, save for mercury compounds, have a straight band gap. They are popular for short wavelength applications in optoelectronics because they typically have significant band gaps. These compounds have band gaps that span the whole band gap (Eg) range, from hexagonal ZnS (Eg = 3.94ev) to semimetals (Eg = 0ev) for the majority of mercury compounds [7]. Group IV metals and group VI chalcogens, including PbTe, SnTe, GeTe, PbSe, and PbSe, are the building blocks of IV-VI semiconductors, which are designated AIV BV I. These compounds are among the most significant classes of semiconductors, with an average of five valence electrons per atom. Some of these compounds, such P bS, are well-known for their use in infrared detectors.

Chapter one:

Table(I.1): Compound semiconductor materials listed by group and in order of increasing band-gap energy ranging from the near-IR to XUV wavelengths.

Band-	Elemental	Binary IV-	Binary III-	Binary II-	Binary IV-VI	Binary n–	Ternary
gap	group	IV	V	VI	compounds	VIIB	compound
energy	IVB	compounds	compounds	compounds		compounds	
(eV)							
0.00-	Sn		InSb ⁺	НgТе			HgCdTe
0.25							
0.25-		SiGe	InAs	HgSe	PbSe;PbS;PbTe		
0.50							
0.50-	Ge [‡]		GaSb				
0.75							
0.75-		SiGe					InGaAs
1.00							
1.00-	Si [‡]				SnS		
1.25							
1.25-			GaAs [‡] ,	CdTe [‡]			AlInAs
1.50			InP [‡]				
1.50-			AlSb	CdSe [‡]			AlGaA
1.75							
1.75-			BP, InN			BiI3 [†]	CdZnTe [‡] ,
2.00							CdZnSe [‡] ,
							InAlP

I.4. Presentation of Nickel sulfide

Because of its high electron mobility, strong infrared reflection, ease of manufacture, and low toxicity, nickel sulfide is the most appealing material. Nickel sulfides, one of the primary classes of transition metals, are found in many phases, including NiS, NiS2, Ni3S2, Ni7S6, and Ni9S8. The increasing demand for energy storage systems should be met by NiS's exceptional capacity performance and high redox activity among these phases [8]. This material is considered tough and significant by scientists. NiS typically occurs in two phases:

Chapter one:

rhombohedral and hexagonal [9]. There are several uses for both phases. Various techniques such spray pyrolysis [10], chemical bath (CBD) deposition [11], hydrothermal [12], Thin films of NiS have been deposited via sol-gel [13], electro-deposition [14], thermal evaporation [15], and successive ionic layer (SILAR) adsorption and reaction [16]. Since thin films are crucial for industrial production, a simple and affordable method should be sought out. One such method that has shown promise is the spray pyrolysis method, which requires only basic equipment and inexpensive films rather than sophisticated technologies and complicated equipment. Strong adherence to the substrate, the capacity to create films with comparatively wide surfaces, and the ability to produce films meeting the necessary specifications are the characteristics of these films deposited in this manner. This is accomplished by combining a solution of two or more components and changing the proportions involved in the composition of the film.

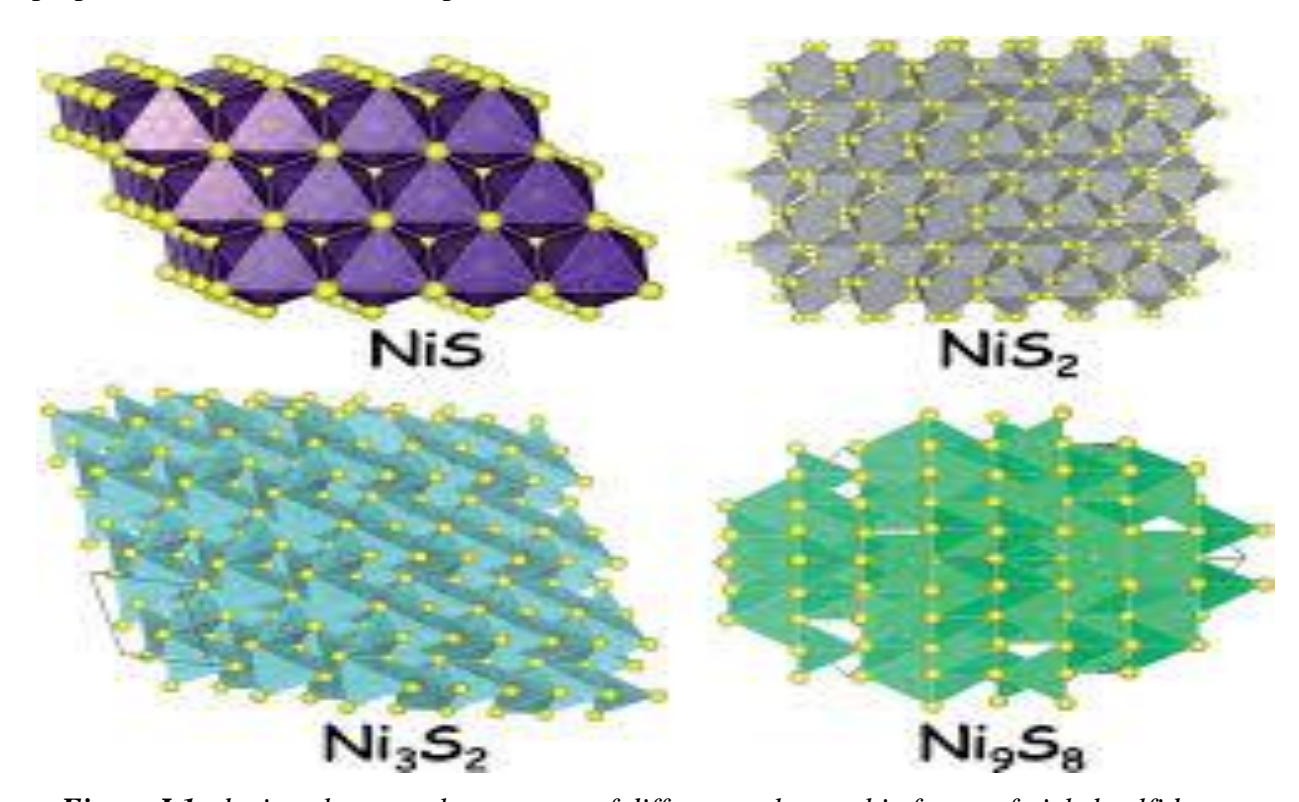


Figure I.1: depicts the crystal structures of different polymorphic forms of nickel sulfides.

I.4.1. Structural Properties

There are two different stoichiometric phases in which nickel sulfide crystallize. The first, the α-NiS phase, is noticeable at high temperatures and has a hexagonal shape. In transition metal chemistry, this phase is regarded as important. Known as millerite, the second phase, β -NiS, has a rhombohedral structure and occurs at lower temperatures [17]. The ternary crystal structure of the odorless, naturally occurring mineral millerite has the R3m space group. Because of this property, nickel sulfide is a stable and appropriate option for electrocatalytic water splitting in alkaline, neutral, and near-neutral conditions. During the metal-semiconductor transition, **Jeffrey et al.** [18] measured the intensity of the X-ray diffraction peak in hexagonal nickel sulfide metal at both high and low temperatures. Studying the atomic locations in both phases was their aim. In the semiconducting phase, they saw a shift in the unit cell symmetry from P63/mmc to P63mc.

The physical measurements of unit cells within a crystal lattice are referred to as the lattice parameter. Three lattice constants, denoted by the letters a, b, and c, are commonly found in three-dimensional lattices. Only the a and c constants are mentioned in hexagonal phase crystal formations, though, because there is a unique situation in which the a and b constants are equal. Similarly, just the a constant is mentioned in rhombohedral phase crystal formations, where all a, b, and c constants are equal. However, the three lattice constants and the three angles between them are part of the complete set of lattice parameters. The crystallographic parameters for the hexagonal crystal system are as follows: a = b = 3.420 Å, c = 5.300 Å, with Alpha (°) = Beta (°) = 90° and Gamma (°) = 120°, as recorded in the ICSD 98-060-2488 card.

The **Table (I.2)** below reviews various works and research studies focusing on the crystallite size and structural phases of nickel sulfide prepared using different methods.

Table (I.2): The preferred orientation, Structure and Crystallite size of various deposited NiS thin films [19].

Phase	Condition	Preferred	Structure	The Crystallite
		orientation		size
NiS	T=250°C,[NiCl ₂ ,2H ₂ O]=	(100)	Hexagonal	29.997 nm
	10^{-2} M [S=C(NH ₂) ₂]=2. 10^{-2} M			
NiS	$[C_4H_6O_4Ni.4H_2O]=0.07M$	(012)	Hexagonal	19.573 nm
	$[CS(NH_2)_2]=0.21M,$			16.796 nm
	T=300°C, Annealing time			23.500 nm
	(0h, 1h, 2h &3h at 300°C			16.795 nm
NiS	[Ni(NO ₃) ₂ .6H ₂ O]/	(010)	Hexagonal	23.903 nm

	$[CS(NH_2)_2]=1/3$, Ionized			27.519 nm
	water=150ml, [C1=0.03M,			42.678 nm
	C2=0.05M, C3=0.07 M],			
	T=300°C			
β-NiS	Ni(acac) ₂] as nickel & H ₂ S	(300)	Rhombohedral	
	gas as sulfur precursors.			/
	T=200-240 °C			
β-NiS	bis(2.2,6.6	without any	Rhombohedral	/
	tetramethylheptane-3.5			
	dionate) nickel(II) [Ni(thd) ₂]			
	& hydrogen sulfide (H ₂ S)			

I.4.2. Optical Properties

One of the best ways to comprehend and increase our grasp of the band structure and energy band gap is to analyze the optical observation spectrum (Eg). A UV-Vis-NIR spectrophotometer was used for optical characterization. The wavelength range used to analyze NiS's optical absorbance spectrum was 200 nm to 900 nm. Three areas were identified within this range: the visible ($\lambda = 380-740$ nm), the UV ($\lambda = 280-380$ nm), and the near-IR ($\lambda = 740-900$ nm). The photoluminescence (PL) characteristics of NiS nanoparticles implanted in a silica gel matrix were examined by **Yang et al.** [20]. According to their findings, the PL spectrum showed two separate emission peaks: one that emerged at 440 nm when stimulated at 380 nm and another that emerged at 610 nm when excited at 490 nm. The NiS nanoparticles in the silica gel's porous structure are responsible for this distinct emission characteristic. However, **Sartale et al.** [21] used the SILAR approach for deposition on both glass and glass substrates covered with FTO to explore the production of NiS thin films. According to their optical measurements, the films' optical band gap and activation energy were 0.45 eV and 0.15 eV, respectively. The optical band gap values for NiS thin films are reported to range from the data listed in Table (I.3).

Table (1.3): The transmittance /absorbance and the optical band gap (Eg) of various deposited NiS thin films.[19]

Phase	Condition	Transmittance	The optical band gap
		/absorbance	(Eg
NiS	T=250°C, [NiCl ₂ ,	T= 20 %	0.55 eV
	$2H_2O]=10^{-2}M$		
	$[S=C(NH_2)_2]=2.10^{-}$		
	2 M		
NiS	T= 325°C, (Ni	T=0.62%	1.03 Ev
	$(NO_3)_2.6H_2O10^{-1}M),$		
	$(SC(NH_2)_2 \ 2.10^{-1} \ M)$		
NiS	/	T=0.62%	1.03 eV
NiS2	T= 55°C (Annealed		1.8 eV 3.1 eV 2.0
	at temperatures of		eV 2.6 eV
	100°C, 200°C,	/	
	300°C and 400°C)		
	NiCl ₂ ,		
	Na ₂ S ₂ O ₃ .5H ₂ O, NH ₃		
NiS2	T= 40°C,		1.22eV 1.20 eV 1.17
	(NiSO ₄ .6H ₂ O),		eV 1.15 eV
	$(Na_2S_2O_3.5H_2O),$	/	
	Deposition Time		
	(10, 15, 20, 25min)		

I.4.3. Electrical properties

Because nickel sulfide thin films could be used in a variety of electronic devices, it is imperative to investigate their electrical characteristics. The synthesis process and the particular circumstances in which the films are made might affect characteristics including conductivity, resistance, and dielectric behavior. However, **Basha et al.** [22] used chemical bath deposition at 80 °C for 60-minute periods to successfully generate NiS thin films on glass substrates. The results of their electrical measurements showed that these films'

conductivities ranged from 1.35 to 48.3 S/cm. According to **Boughalmi et al's** research, this conductivity range indicates their appropriateness for solar cell applications and their potential efficacy in them [23]. centered on the metallic properties of thin films of nickel sulfide produced at 250 C° using the spray pyrolysis method. They discovered that the conductivity of the direct current exhibited metallic characteristics. Furthermore, studies of the Hall effect at 24C° revealed a negative Hall coefficient, which is a sign of electronic conductivity, along with an electron mobility of roughly 0.6 cm2/Vs and a charge carrier density of about 3.67×1022 cm-3. Additionally, their theoretical model demonstrated that the density of states and structural characteristics of NiS support the metallic behavior, which is consistent with experimental findings.

I.5. Nickel sulfide applications

I.5.1. Electrodes of LIBs and Supercapacitors (SCs)

Conversion-reaction-based metal sulfides (M–S, where M = Fe, Co, Ni, etc.) offer high theoretical capacities for lithium storage due to redox reactions. However, sulfide anodes face challenges like electrode pulverization, leading to rapid capacity decline [24]. Supercapacitors, known for their high capacitance but lower voltage limits, bridge the gap between electrolytic capacitors and rechargeable batteries. They store energy through double-layer capacitance and pseudocapacitance, offering high energy density and robust cycle stability. Their affordability also makes them attractive for applications requiring fast charging and discharging [25].

Nickel sulfides can serve as both cathode and anode materials in lithium-ion batteries (LIBs). Under deep discharge, they react with Li⁺ to form metallic Ni and Li₂ S, showing promising theoretical capacities. Reported capacities for NiS, Ni₂ S₃, and Ni₃ S₄ are 590, 445, and 704 mAh g⁻¹, respectively. However, their utilization rate in LIBs is relatively low [26]. Kumar et al. [27] employed the SILAR technique on a nickel foam base, creating NS-SnS (NTS) heterogeneous electrodes for asymmetric supercapacitors. These electrodes showed an impressive specific capacitance of 1653 F g⁻¹ at 1 A g⁻¹, high energy density (83 Wh kg⁻¹), and power density (117 W kg⁻¹), with superior rate performance and stability over multiple cycles.

I.5.2.Oxygen Reduction Reaction (ORR)

It can be challenging to produce nickel sulfide using certain surface site compositions or shapes, such as compatible thin films, due to its high stability, superconductivity, and ability to chemically reduce protons to hydrogen gas as efficiently as pricey noble metals [28]. Yasemin et al. [28] assessed the electrocatalytic activity of NiSx prepared using the ALD technique for molecular hydrogen evolution. Films were cultivated on supports made of conductive glass. With extremely low NiSx loading, the overvoltage was measured at a current density of 10 mA/cm2 in both acidic aqueous reaction media and phosphate buffer of pH 7. It was discovered to be 440 and 576 mV, respectively. These findings suggest that NiSx materials generated via ALD have potential as water-compatible electrocatalysts.

Films were cultivated on supports made of conductive glass. In both acidic aqueous reaction media and phosphate buffer with a pH of 7, the overvoltage was measured at a current density of 10 mA/cm2 and was discovered to be 440 and 576 mV, respectively, with very low NiSx loading. These findings suggest that NiSx materials generated via ALD have potential as water-compatible electrocatalysts.

I.6.Semiconductors Doping

N-type doping is the process of creating an overabundance of negatively charged electrons. P-type doping is the process of producing an excess of holes, which are thought to be positively charged, by causing an electron deficit.

Donor and acceptor atoms

The impurity atom and the atom it replaces are from the same period and group in Mendeleev's periodic table [29]. The dopant atom is isovalent (or iso-electronic) if it is a member of the same group as the parent atom. In this instance, the material's electrical conduction characteristics are unaffected, and the impurity atom's valence electrons precisely replace the original atom's.

The dopant atom lacks one peripheral electron necessary to complete all of the initial covalent bonds if it is a member of the previous group. Since the atom can take on an additional electron to fill the valence band, it is referred to in this context as an acceptor (of electrons). P-type is the name given to such an atom.

In comparison to the original atom, the dopant atom contains one extra peripheral electron if it is a member of the following group. The first covalent connections are In these

bonds, one electron is not utilized. As a result, it is in a free state inside the system. We refer to the inserted atom as a donor (of electrons). This doping is of the N-type.

It is said to as amphoteric when the same doping atom can act as both a donor and an acceptor. For instance, silicon (Si, column IV), a dopant in gallium arsenide (AsGa), functions as an electron donor if it replaces a gallium atom (column III). It functions as an acceptor if it replaces an arsenic atom (column V). The impurity atoms are ionized at room temperature if the ionization energy ΔE is less than the ambient thermal energy kT, where T is the temperature and k is the Boltzmann constant.

I. 7. Thin Film Deposition Methods

Thin film deposition is the technique of applying a thin layer of one substance over another. The underlying substance on which the layer is applied is known as the substrate, and the layer itself is known as a thin film. Thin films have become an important component of microelectronic circuitry due to their modest thickness, i.e. a practically two-dimensional structure that allows for the manufacture of extremely small devices or microcircuits [30]. Thin film deposition techniques are simply classified into two types: (1) physical vapor deposition and (2) chemical vapor deposition. However, a significant number of deposition methods use both physical and chemical processes [31].

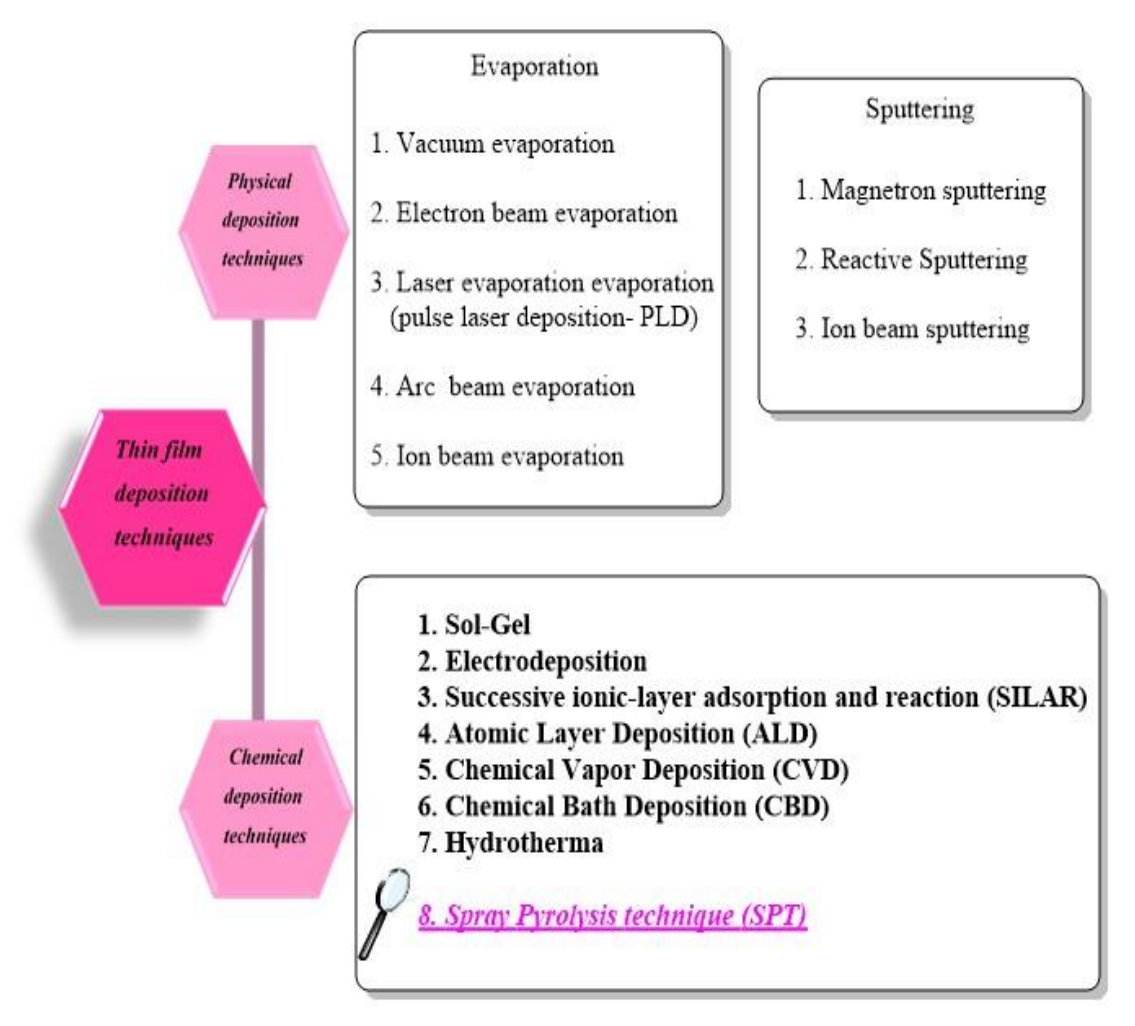


Figure (I.2): Categorization of thin film deposition methods.[19]

I. 7.1. Pulsed Laser Deposition (PLD)

This technology uses high-power short pulsed laser irradiation of solid targets to remove material from the targeted zone by physical vapor deposition [32]. PLD is a relatively recent but highly efficient technology for depositing epitaxial layers. It is a very expensive method, but it can generate high-quality films with precise thickness control [33]. However, repeatability, large-area deposition, and particle emission reduction all need to be improved [32].

I. 7.2. Sputtering

This approach removes atoms from the object by blasting it with high-energy particles. The cathode is the substance to be deposited, whereas the substrate is referred to as the anode [32]. Sputtering is a cost-effective alternative to PLD and allows for large-area deposition [33].

I. 7.3. Thermal Evaporation

The technique involves evaporating source materials in a vacuum chamber and condensing them on a substrate. Conventionally, thermal evaporation is referred to as vacuum deposition. Due to the use of resistive heating, this approach is not suitable for high melting point materials or weak thermal conductors [34, 35].

I. 7.4. Chemical Vapor Deposition (CVD)

Chemical vapor deposition is the technique of allowing non-volatile gas phase reaction products to deposit onto a substrate [36]. CVD is a versatile synthesis method that can easily produce both simple and complicated molecules. Fundamental CVD concepts span a wide variety of disciplines, including gas-phase reaction chemistry, thermodynamics, kinetics, transport processes, film growth phenomena, and reactor engineering [37]. CVD offers advantages such as high deposition rates, cheap cost, and flexibility in composition management. CVD may not be acceptable for substrates that are thermally unstable at high temperatures due to the high deposition temperature [37].

I. 7.5. Spin Coating

The spin coating technique involves depositing droplets of liquid precursor on the surface of a spinning substrate [38]. The film created on the substrate is a result of two balancing forces: centrifugal force (from spinning) driving the viscous sol outwards and viscous force (from friction) acting radially inwards [39]. Spin coating is the least expensive film manufacturing process in silicon technology [40]. Thinner films (<100 nm) are challenging to produce and can squander 98% of the process resources [41].

I. 7.6. Spray deposition method

The structure and characteristics of films are largely determined by synthesis techniques. One of the most significant techniques for creating thin nickel sulfide films and their composites to date is spray pyrolysis. Because of its ease of use, processing versatility, and capacity for precise production control, this method has become increasingly popular. We will apply nickel sulfide thin films using the spray pyrolysis technique to produce nickel sulfides with the appropriate shape and controllable size. The next chapter will go into more detail about this procedure.

I. 8.Fluoride

I. 8.1. Definition

Fluorine is a chemical element with the symbol F, derived from the Latin "fluere" and the Greek "fluein". It exists in the form of a diatomic gas (F_2) , characterized by a pale yellow color under standard conditions of temperature and pressure. Fluorine is a toxic gas with harmful effects on living organisms. It has an atomic number of 9, and its electronic configuration is $(1s^2\ 2s^2\ 2p^2)$, meaning that two electrons occupy the inner shell, while seven electrons are in the outer shell. This indicates that fluorine needs one more electron to complete its outer shell, which explains its high chemical reactivity. Fluorine is located at the top of the halogen group in the periodic table and is known as the most electronegative element, enabling it to form chemical compounds with almost all elements even with some noble gases. The salts derived from fluorine are known as fluorides [42].

I.8.2. The physical properties of fluoride

Table (I.4): The physical properties of fluoride

The property	The value
Atomic mass(g.mol/1)	18,998
The density of the liquid at the boiling point(g.cm/3)	1,50
Melting point(C°)	-219,62
Boiling point(C°)	-188,2
Electronic intima kcl/mol	79,6
Homelessness constant ev	17,42
Bond length F_F(A°)	1,42
Dissociation energy kcl/mol	38,3
Heat of vaporization kcl/mol	0,755
Critical pressure(atm)	55
Critical temperature(C °)	-196

I. 9. Conclusion

This work presents a comprehensive study of nanostructured thin films, focusing on the semiconductor material nickel sulfide (NiS). The structural, optical, and electrical properties of these thin films were examined, highlighting their various applications in advanced technology. Thin films play a crucial role in the development of electronic and optical devices, as their unique properties enable performance enhancement in applications such as solar cells, sensors, and nanoelectronics. Additionally, controlling the properties of these materials through manufacturing processes and doping represents a significant step toward improving their efficiency and expanding their future applications. Based on the presented discussion, it can be concluded that ongoing research in thin films and their property optimization can lead to major advancements in technological and scientific industries, enhancing device efficiency and contributing to sustainable innovation.

References

- [1] Baedeker K. Electrical conductivity of thin metallic films. Ann Phys. 1907;22:749–66.
- [2]Jana S, Mukherjee N, Chakraborty B, Mitra BC, Mondal A. Electrodeposited polymer encapsulated nickel sulphide thin films: Frequency switching material. Appl Surf Sci 2014;300:154–8.
- [3] Chopra KL. Thin-Film Phenomena. New York: McGraw-Hill; 1969.
- [4] Paulson PD, Chopra KL, Dutta V. Thin-film solar cells: an overview. Prog Photovolt Res Appl. 2004;12:69–92.
- [5] Kumar S, Aswal DK. Thin film and significance of its thickness. In: Kumar S, Aswal DK, editors. Recent Advances in Thin Films. Singapore: Springer; 2020.
- [6] Owens A. Semiconductor materials and radiation detection. J Synchrotron Radiat. 2006;13(2):143–50.
- [7] Klingshirn C. Zinc Oxide: From Fundamental Properties to Modern Applications. Berlin: Springer; 2010.
- [8] Yu SH, Yoshimura M. Adv Funct Mater. 2002;12(4):277.
- [9] Zhang Y, Peng Z, Guan S, Fu X. Data Brief. 2018;16:828.
- [10] Gahtar A, Benramache S, Ammari A, Boukhachem A. Ann West Univ Timisoara-Phys. 2021;63(1):1.
- [11] Suresh S, Anand SS, Arul R, Isha D. Chalcogenide Lett. 2016;13(7):291.
- [12] Patil A, Lokhande A, Shinde P, Kim J, Lokhande C. J Energy Chem. 2018;27(3):791.

- [13]Yang P, Lü M, Song CF, Zhou G, Xu D, Yuan DR. J Phys Chem Solids. 2002;63(11):2047–51.
- [14]Ruan H, Li Y, Qiu H, Wei M. J Alloys Compd. 2014;588:357.
- [15]Singh RK, Narayan J. Phys Rev B. 1990;41(13):8843.
- [16]Sartale S, Lokhande C. Mater Chem Phys. 2001;72(1):101.
- [17] Pothu R, Bolagam R, Wang QH, Ni W, Cai JF, Peng XX, et al. Nickel sulfide-based energy storage materials for high-performance electrochemical capacitors. Rare Met. 2021;40:353–73.
- [18] Trahan J, Goodrich R G WSF. X-Ray Diffraction Measurements on Metallic and Semiconducting n.d.
- [19] Sbaihi A. Enhancement of superconducting properties of MgNiS by using oxygen annealing atmosphere [dissertation]. Biskra (DZ): University of Mohamed Khider of Biskra; 2024.
- [20] Yang P, Lü M, Song CF, Zhou G, Xu D, Yuan DR. J Phys Chem Solids. 2002;63(11):2047–51.
- [21] Sartale SD, Lokhande CD. Preparation and characterization of nickel sulphide thin films using successive ionic layer adsorption and reaction (SILAR) method. Mater Chem Phys. 2001;72(1):101–4.
- [22] Basha KAJ, Guddeti PR, Kotte TRR. Effect of deposition time on the properties of NiS films. Indian J Sci Technol. 2022:2492–9.
- [23] Boughalmi R, Rahmani R, Boukhachem A, Amrani B, Amlouk M. Metallic behavior of NiS thin film under structural, optical, electrical, and ab initio investigation frameworks. Mater Chem Phys. 2015;163:99–106.
- [24] Shi W, Zhu J, Rui X, Cao X, Chen C, Zhang H, et al. Controlled synthesis of carbon-coated cobalt sulfide nanostructures in oil phase with enhanced Li storage performances. ACS Appl Mater Interfaces. 2012;4(6):2999–3006.
- [25] Pothu R, Bolagam R, Wang QH, Ni W, Cai JF, Peng XX, et al. Nickel sulfide-based energy storage materials for high-performance electrochemical capacitors. Rare Met. 2021;40:353–73.
- [26] Jasinski R, Burrows B. Cathodic discharge of nickel sulfide in propylene carbonate-LiClO₄ electrolyte. J Electrochem Soc. 1969;116:422–4.

- [27]Kumar N, Mishra D, Kim SY, Jin SH. Self-assembled nis-sns heterostructure via facile successive adsorption and reaction method for high-performance solid-state asymmetric supercapacitors. Thin Solid Films 2020;709:138138.
- [28] Yasemin C, Peters AW, Avila JR, Ho WL, Goswami S, Farha OK, et al. Atomic Layer Deposition of Ultrathin Nickel Sul fi de Films and Preliminary Assessment of Their Performance as Hydrogen Evolution Catalysts 2016.
- [29] J.L. Santailler, Croissance de monocristaux de ZnO: état de l'art, Journée thématique INP Grenoble Minatec, 2007.
- [30]Arthur JR. Specimen handling, preparation, and treatments in surface characterization. New York: Plenum Publishers; 1998.
- [31] Seshan K. Handbook of thin film deposition: processes and technologies. 2nd ed. New York: William Andrew Publishing; 2002.
- [32] Liu Y, Wang ZL, Zhang Z. Handbook of nanophase and nanostructured materials: vol. 1. New York: Kluwer Academic, Plenum Publishers; 2003.
- [33] Banerjee AN, Chattopadhyay KK. Progress in crystal growth and characterization of materials. 2005;50:52–105.
- [34] Kitabatake M, Wasa K, Adachi H. Thin films material technology: sputtering of compound materials. New York: William Andrew Publishing; 2004.
- [35] Bishop CA. Vacuum deposition onto webs, films, and foils. New York: William Andrew Publishing; 2007.
- [36] Coleman RV, Horovitz KL. Solid state physics. New York: Academic Press; 1974.
- [37]Pierson HO. Handbook of chemical vapor deposition. New York: Noyes Publications; 1999.
- [38] Pauleau Y. Chemical physics of thin film deposition processes for micro- and nanotechnologies. Netherlands: Kluwer Academic Publishers; 2002.
- [39]Mader H, Widmann D, Friedrich H. Technology of integrated circuits. Berlin: Springer-Verlag; 2000.
- [40]Busnaina A. Nanomanufacturing handbook. USA: Taylor & Francis Group; 2007.
- [41] Chopra KL, Das SR. Thin film solar cells. New York: Plenum Press; 1983.
- [42]Kirch P. Modern Fluoroorganic Chemistry. Weinheim: Wiley-VCH; 2004.

Chapter two:

Experimental parts

II. 1.Introduction

Thin films require careful consideration when selecting an appropriate preparation procedure due to their delicate and precise features. Various processes may be used to deposit films of alloys, metals, ceramics, and superconductors on different substrate materials, each with its own advantages and disadvantages. We chose the Spray Pyrolysis Technique (SPT) as a very effective and accurate method for this investigation. SPT is a cost-effective and simple alternative to conventional procedures [1].

II. 2. Generalities of spray pyrolysis technique

This deposition technique involves spraying liquid precursors by atomization and condensing them on surfaces at high temperatures. When sprayed micro-droplets reach the heated substrate surface, they decompose into single or clustered crystallites. Spray pyrolysis was first employed in 1910 to produce transparent oxide films [2]. Spray pyrolysis (SPT) is a good method for creating thin films. In English, "spray" refers to the dispersal of liquids into fine droplets by spraying, such as perfume, deodorant, or pesticide. Pyrolysis comes from the phrase "pyrolytic," which refers to the heating of a substrate. To free a metal or compound, the parent material must undergo heat breakdown. The substrate's temperature provides activation energy, which initiates the chemical reaction between the components. Spray pyrolysis is an effective method for creating thin films, including metal oxides, superconducting materials, and nanophase materials. Spray pyrolysis offers the ability to manufacture materials with varying band gaps. Spray pyrolysis offers versatility in creating large-area films and the ability to manufacture materials with varying band gaps throughout the deposition process [3].

II. 2.1. Advantages of spray pyrolysis Technique

- Simply controllable reaction environment, either in air at atmospheric pressure or in a neutral gas;
- ➤ This kind of reactoriseasy to manufacture.
- ➤ In the case of solar cells or flat screens, these techniques can be utilized to deposit on enormous surfaces.
- > The possibility of preparing many materials.
- **Easy and customizable.**
- This is an inexpensive and economical technology.
- > Simple in implementation and fast.

- An easy way to add precursors by spraying.
- \triangleright This method produces thin films that are of high quality [4,5].

II. 2.2.Disadvantage of spray pyrolysis Technique

While SPT offers a number of benefits, italso has certain drawbacks [6]:

- > SPT offers a reduced yield.
- > It still has trouble determining the growing temperature.
- ➤ Under air environment conditions, sulfide oxidations a possibility.

II. 3.3. Classification & equipment of the Spray Pyrolysis Technique

Spray pyrolysis is a versatile process that may create both powders and porous films. Furthermore, it can produce multilayered films. This method has been used for many years in the glass and solar cell manufacturing industries.

The substrate heater, temperature controller, atomizer, and precursor solution are crucial components of the pyrolysis equipment [7].

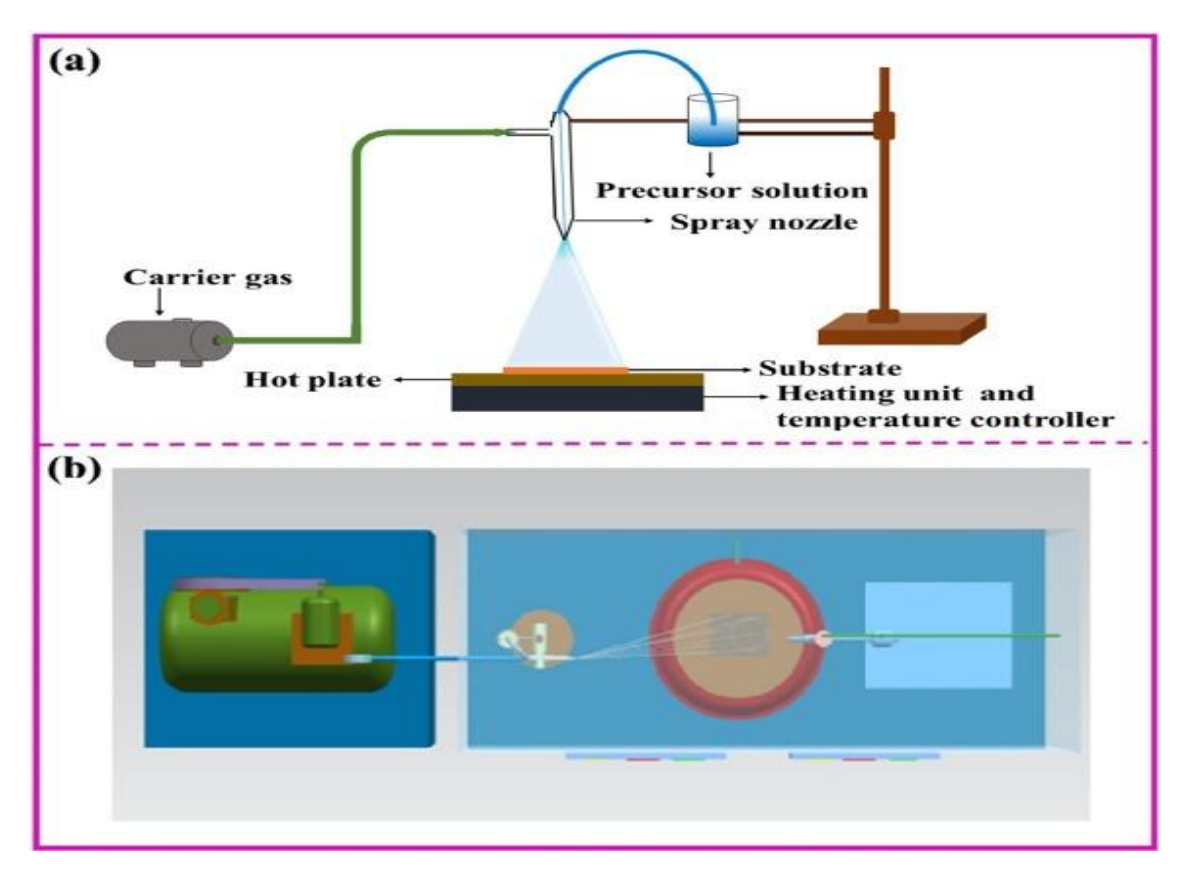


Figure (II.1): Diagrammatic representation of spray pyrolysis equipment.[10]

Spray methods differ based on the energy source utilized to trigger the precursor reaction. Various pyrolysis methods exist, including tube reactor spray, vapor flame spray, emulsion combustion, and flame spray [8].

Precursor atomization techniques vary depending on the technology used, including air pressure, electrostatic forces, and ultrasonic procedures in spray pyrolysis operations [9].

II. 3. Principle of deposition processes in spray pyrolysis

Three phases are the foundation of the spray pyrolysis deposition process, and they can happen concurrently or sequentially during film creation; we propose to classify the processes that occur with increasing temperature see figure (II.2).

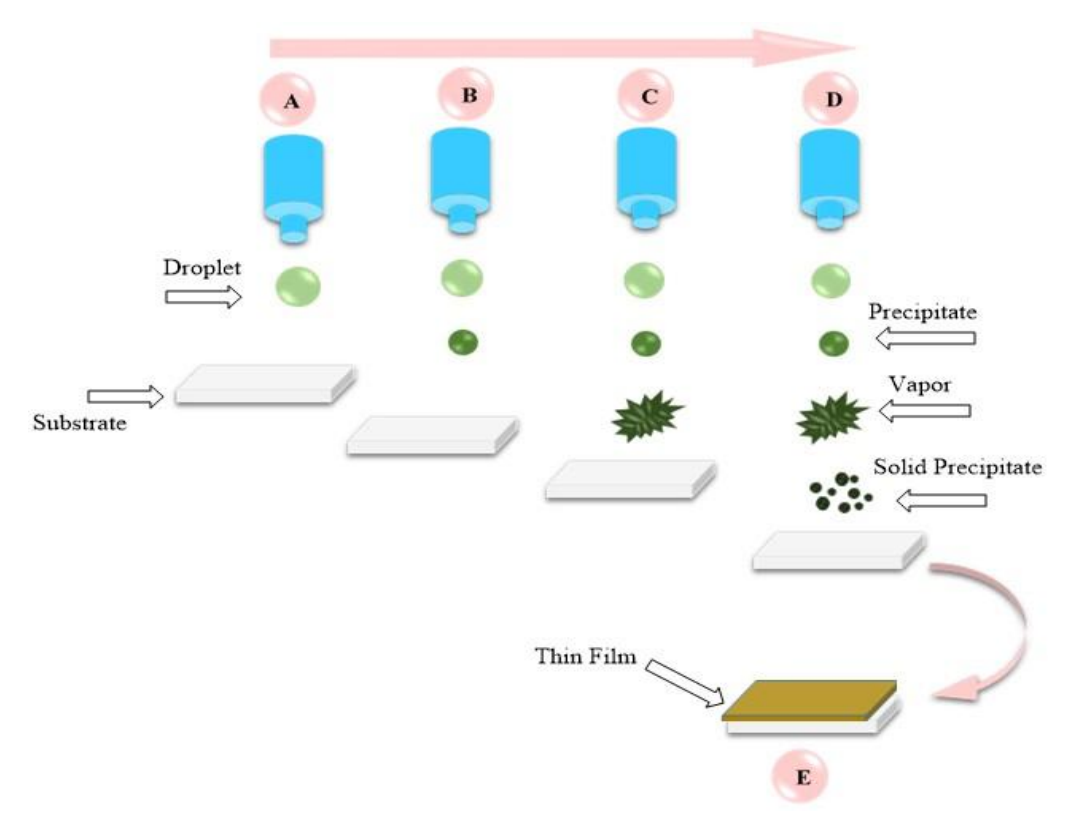


Figure (II.2): Description of the deposition processes [10].

II. 3. 1. Atomization of the precursor solution

Atomization is the first stage in the spray pyrolysis deposition process. The process involves creating spray solution droplets with a high initial velocity and directing them towards the heated substrate. Spray pyrolysis procedures typically use air blast, ultrasonic, and electrostatic sprays [11]

II. 3. 2. Aerosol transport of the droplet

To transfer as many droplets as possible to the substrate's surface without forming powder or salt particles, the raw material is dissolved in a solvent, resulting in fine droplets of appropriate size. These droplets are then transferred to the hot surface using a carrier gas. Droplet transport affects several factors: The thermophoreticforc; the gravitational force; The electric force and The stokes force [10].

II. 3. 3. Decomposition of the precursor to initiate film growth

- ✓ Pyrolysis technology is based on the thermal decomposition of raw materials. To explain this process, we propose to classify the processes that occur as the temperature increases.
- ✓ In Process A, droplets land on the substrate's surface and evaporate, creating a dry precipitate that aids breakdown.
- During In process B, the precipitate decomposes on the surface as the solvent evaporates before the droplet reaches the substrate. When the droplet comes close to the substrate. In process C, the solvent evaporates, the solid melts and evaporates (sublimating), and the vapor diffuses to the substrate, where it participates in a heterogeneous reaction. It is definitely CVD.
- ✓ Process D involves a chemical reaction in the vapor phase, where the metallic compound vaporizes at high temperatures before reaching the substrate [12].

II.4 Protocol methodology

II. 4. 1. Preparation of spray solution

In the beginning, we prepared a pure spray solution of nickel sulfideNiS by dissolving an amount of nickel nitrate hexahydrate (Ni(NO₃)₂.6H₂O) and thiourea (CS (NH₂)₂) as a source of nickel Ni and sulfur S, respectively in distilled waterwith mass measurement according to the N° 1 formula. The mixture was stirred continuously at 60 °C for 2 hour on a magnetic stirrer leading to the formation of a clear green and homogeneous solution. to prepare the fluoride F doping solution we kept the same conditions and used Fluoride nitrate (NH₄F) as the precursor F molar ratio chosen $x=[S^{-2}]/[F^{-2}]$ varies from 1% to 3% &5%, as shown in figure (II.3).

$$m(g) = C(mol/l).V(l). M(g/mol)$$
 N° (II.1)

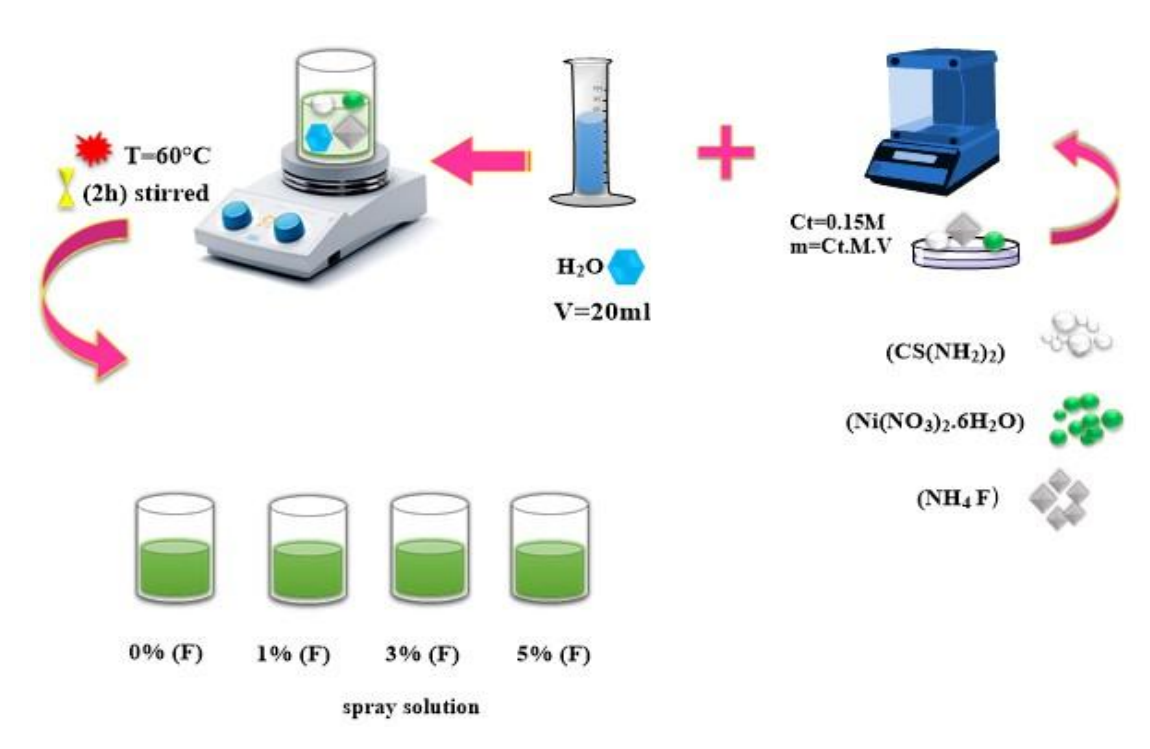


Figure (II.3): Description of the Preparation of the spray solution doped with F.

II. 4. 2. Preparation of thin Films

The type of substrate must be chosen before the films may be deposited. We utilized the glass—substrate—CAT.NO.7101—microscope—glass—slide,—see—figure—(II.4). We rinsed with distilled water and scrubbed thoroughly with acetone and ethanol for 5 minutes each. The substrate was heated on a plate using a Four at 250 °C. The spray pyrolysis process (figure—II.2) was used to create thin films of pure nickel sulfide doped with magnesium.



Figure (II.4): CAT.NO.7101 microscope glass slide.[10]

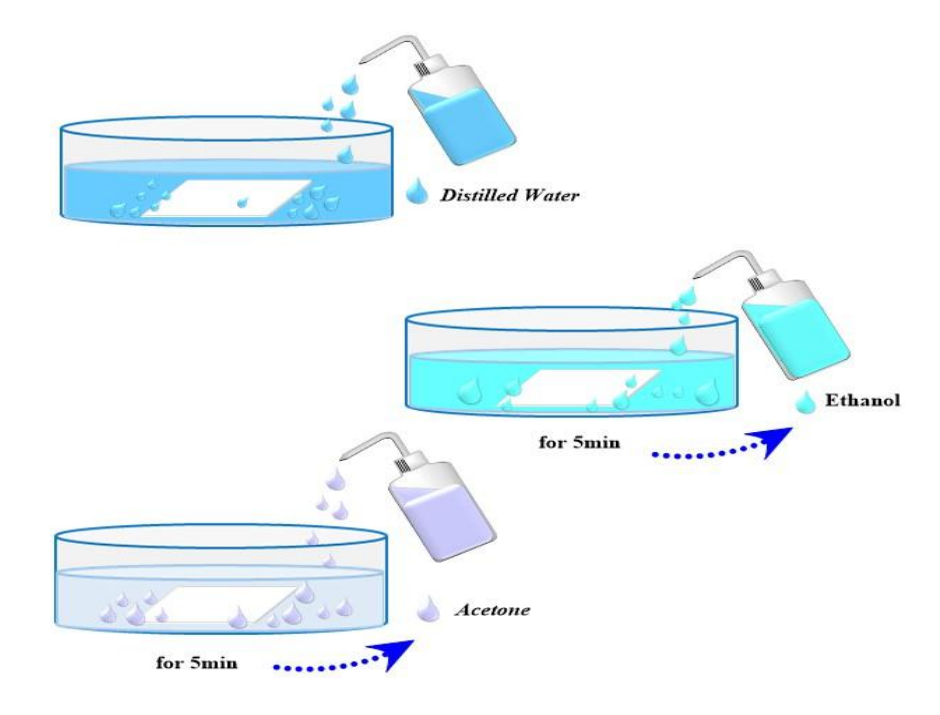


Figure (II.5): Preparation of glass substrates [10]

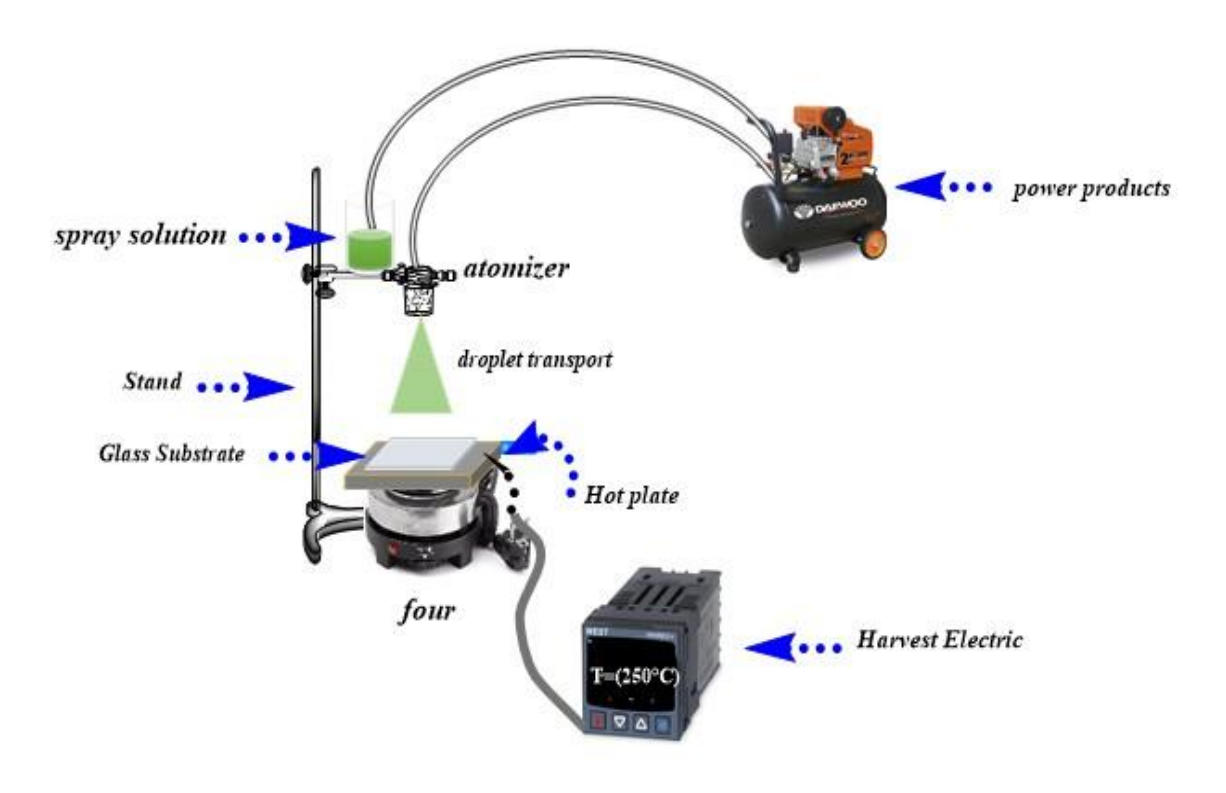


Figure (II.6): Description of the Preparation of thin films by (SPT) [10]

II. 5. Characterization methods

II. 5. 1. X-Ray diffraction technique

This technique uses X-ray diffraction to characterize crystalline materials. It is crucial for evaluating thin films and understanding the crystal structure, atomic arrangement, and crystalline dimensions. This easy and non-destructive sample examination approach determines factors including crystallinity and grain orientation.

A variety of analytical methods were used to characterize thin films. The XRD diffractogram was acquired using a DRX Malvern Pnm analytical Empyrean system and a CuKa radiation source ($\lambda = 0.15406$ nm) in the range of 30°-80°.

Analysis conditions:

Scanning area in (°) 2 Θ i:10, 2 Θ f:90 *

Step in (°): 0.002°

Quantity of sample to analyze: 2 g minimum

II. 5. 1.1. The Lattice parameters

Bragg's law equations are used to compute lattice parameters for the current phase's unit cell. The absence of reflection peaks implies the material is amorphous [13].

$$2d_{hkl}\sin\theta = n\lambda \tag{II.2}$$

- d_{hkl} the spacing between the planes in the atomic lattice.
- θ is the angel between the incident ray and the scattering planes.
- n is an integer.

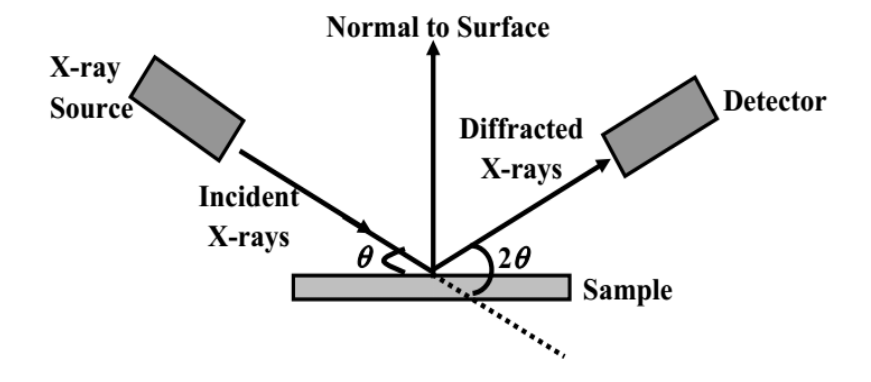


Figure (II.7): Schematic of X-ray diffraction

The lattice parameters define the dimensions of a basic mesh. Our NiS analysis focuses on two parameters, α and c, as shown in figure (II.7). The formula (II.3) is used to calculate the hexagonal lattice parameters (a=b & c) of a nickel sulfide thin film [14].

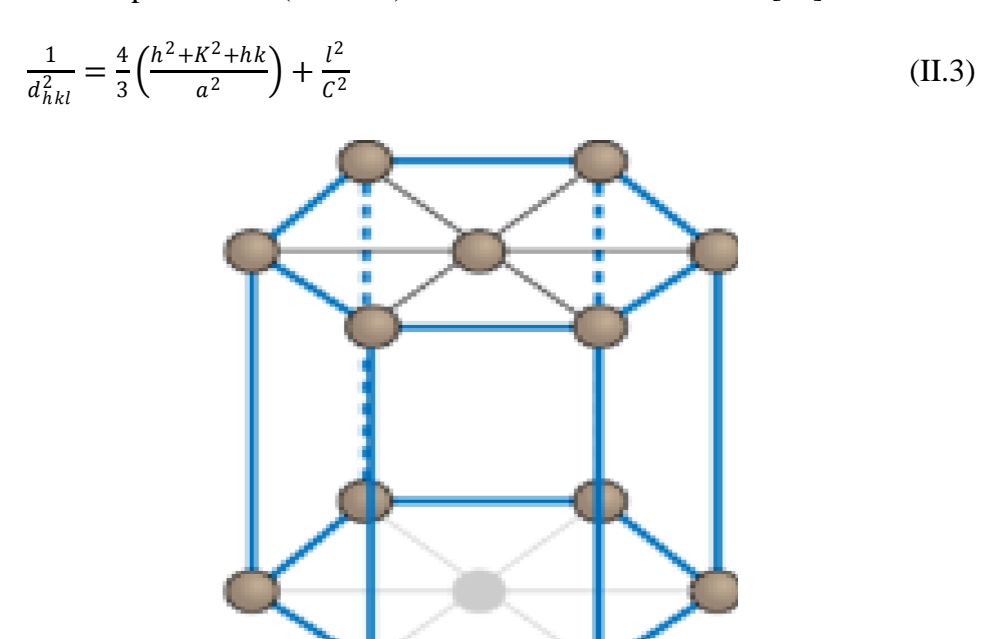


Figure (II.8): Diagram of the hexagonal structure of NiS.

II. 5. 1.2. The Crystallites size (D)

This technology uses a detector to catch diffracted X-rays by scanning over different reflection angles. Data, including intensity levels, are recorded by a computer and shown in figure(II.7). The information is put into a table and compared to ICSD criteria to identify the item under inquiry. The Scherrer equation may be used to determine the size of crystallites from the broadening of the most intense peak, known as the full width at half maximum (FWHM), regardless of the sample type (powder, single crystal, or thin film) [7]. The Debye–Scherrer's equation was used to calculate the crystallite size [15]:

$$D_{hkl} = \frac{k\lambda}{\beta \cos \theta} \tag{II.4}$$

Where:

- β (rad) is full width at half-maximum FWHM.
- θ is the half diffraction angle of the centroid of the peak.

- λ is the wavelength of X-ray ($\lambda = 1.5406 \text{ A}^{\circ}$).
- k is a constant (k =0.89).

II. 5. 1. 3. The dislocations density

A dislocation is a defect in crystals induced by lattice misregistration in one place against another. Dislocations, unlike vacancies and interstitial atoms, are not equilibrium faults, hence thermodynamic methods cannot explain their relevance [16].

 $\delta_{h\,kl}$ represents the dislocation density, itiscalculated using the following relation [17]:

$$\delta_{hkl} = \frac{1}{D^2} \tag{II.5}$$

II. 5.2. Spectroscopy UV-VISIBLE

The optical properties of NiS thin films were measured by a UV-visible spectrophotometer (PERKINELMER Lambda 35) at room temperature in a wavelength range of 200–1200 nm. (The characterization of the samples was performed at the laboratory, Biskra) as shows in figure (II.9).

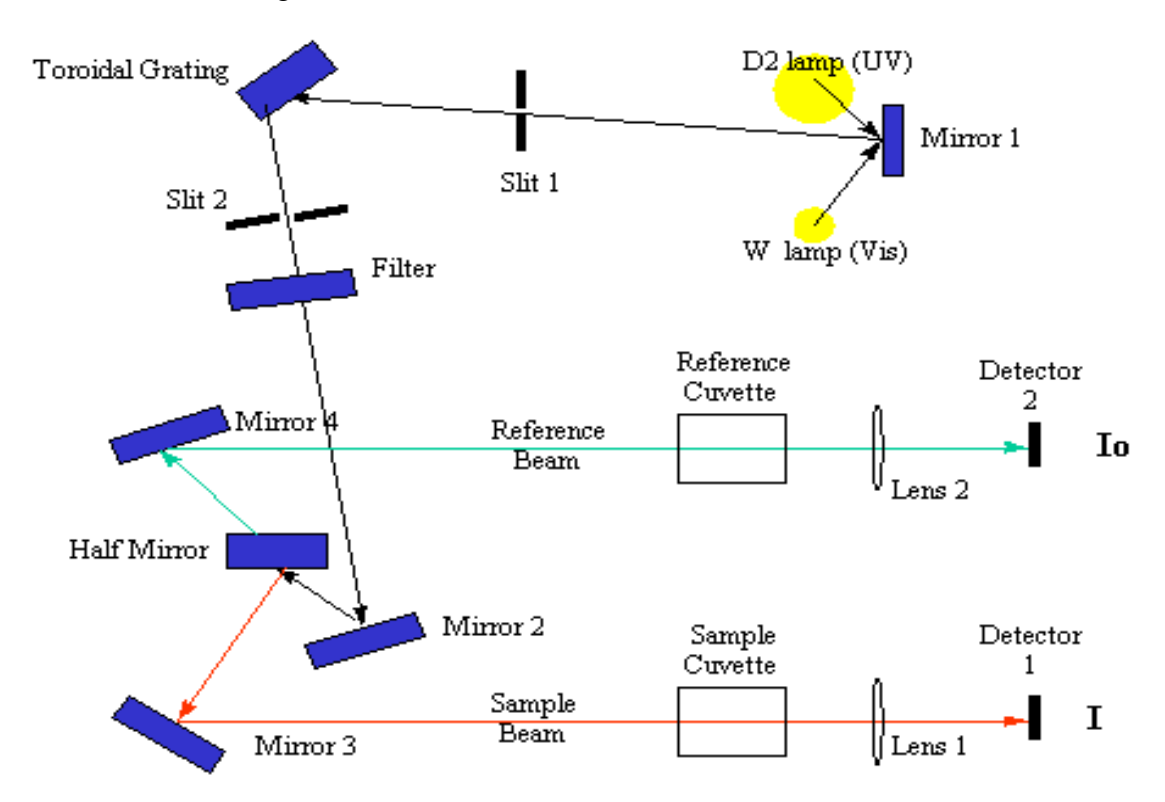


Figure (II.9): The principal operation of UV–Visible spectrophotometer [10]

Principle

The basis of UV-VIS spectroscopy is the idea that, when a monochromatic light beam travels through a homogeneous medium composed of an absorbing material, the rate at which the radiation intensity drops in relation to the absorbing medium's thickness is directly proportional to the medium's concentration as well as the incident radiation intensity [18]:

$$I = I_0 \exp\left(-\alpha t\right) \tag{II.6}$$

Where:

- α is the absorption coefficient.
- I_0 and I are the intensity of the incident and transmitted beams, respectively.

The absorption coefficient (α) can be calculated using the following expression :

$$a = \frac{1}{t} \ln(\frac{100}{T(\%)}) \tag{II.7}$$

Where:

 \bullet T(%) is the transmittance (quantity of the transmitted light), and can be directly measured by:

$$T(\%)=I/I_0.100$$
 (II.8)

The optical band gap energy $(\mathbf{E}\mathbf{g})$ of NiS thin films was derived from the transmission spectra through the utilization of the following relations [19]

$$A = \alpha t = -\ln(T) \tag{II.9}$$

$$(Ahv)^{2} = B(hv - Eg)/A = \alpha t$$
 (II.10)

Where:

- A is the absorbance.
- B is a constant.
- (hv) is the photon energy $1240/\lambda(nm)$ (eV)
- (Eg) is the band gap energy.

On the other hand, we can determine the Urbach energy through the following equation [20]:

$$A = A_0 exp(hv/Eu)$$
 (II.11)

Where:

- A₀ is a constant
- E_u is the Urbach Energy, by plotting Ln(A) in terms of hv, we can ascertain the value of Eu as the reciprocal of the linear tangent that intersects the photon energy at x=0.

II. 5.3. Four-probe method

A diagram of the four-point method with four equally spaced probes composed of a heat-resistant material is shown in Figure (II.10). The motorized mechanical stage on which these probes are mounted can be adjusted vertically, ensuring steady contact with the film for precise measurements.

A four point measurement technique can be used to find the electrical conductivity of the resistivity of a material with a fixed known thickness t using this technique, a fixed DC current I is forced through two of the material's ports, and the DC voltage V at the other two ports is then measured. The arrangement consists of four high temperature points that are uniformly separated from one another. The following formula is then used to determine the thin film's sheet resistivity [21]:

$$R_{Sh} = \frac{\pi}{\ln(2)} \times \frac{V}{I} \& \sigma = \frac{1}{\rho} = \frac{1}{t \times RSh}$$
 (II.12)

Where:

- • R_{Sh} is sheet resistivity.
- σ is electrical conductivity.
- ρ is the electrical resistivity.
- t is the film thickness.
- I is the applied current.
- V is the measurement voltage.

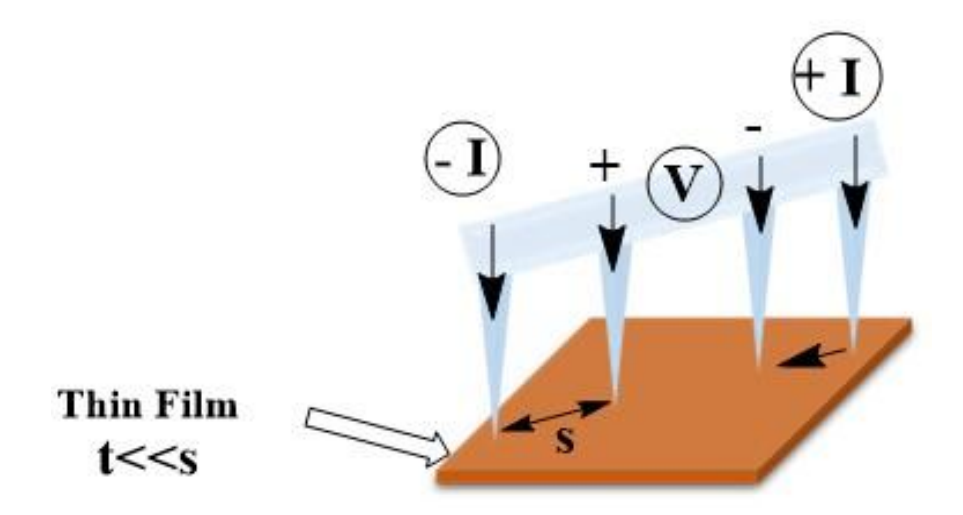


Figure (II.10): Schematic of four point method

II. 5. 3. Fourier Transform Infrared Spectroscopy (FTIR)

An infrared spectrometer of (type Perkinelmer Spectrum Two) was used in the frequency range of 400–4000 cm-1 at room temperature to study the chemical bonding properties of the prepared films. (This was performed at the Laboratory in Biskra).

Principle

One of the most versatile analytical techniques for the non-destructive chemical characterization of samples is Fourier transform infrared spectroscopy (FTIR). It could provide fundamental details about the molecular makeup of both organic and inorganic substances. Changes in quantized vibrational energy levels are connected to the basic operating concept of the FTIR method. An IR photon transfers to a molecule in FTIR analysis, stimulating it to a higher energy state. The absorption of infrared radiation is the term for this process.

Molecular bond vibrations, including as stretching, bending, twisting, rocking, wagging, and out-of-plane deformation, take place at various wave numbers (or frequencies) in the infrared portion of the light spectrum due to the excited states. The intrinsic physicochemical properties of the corresponding molecule determine the wavenumber of each IR absorbance peak [22]. Band intensities in the infrared spectrum can be represented as either absorption (A) or transmittance (T). A range of bands in the infrared spectrum indicate the distinctive functional groups and bonds present in a chemical compound, and these bands can be used as a fingerprint to identify the molecule [23]

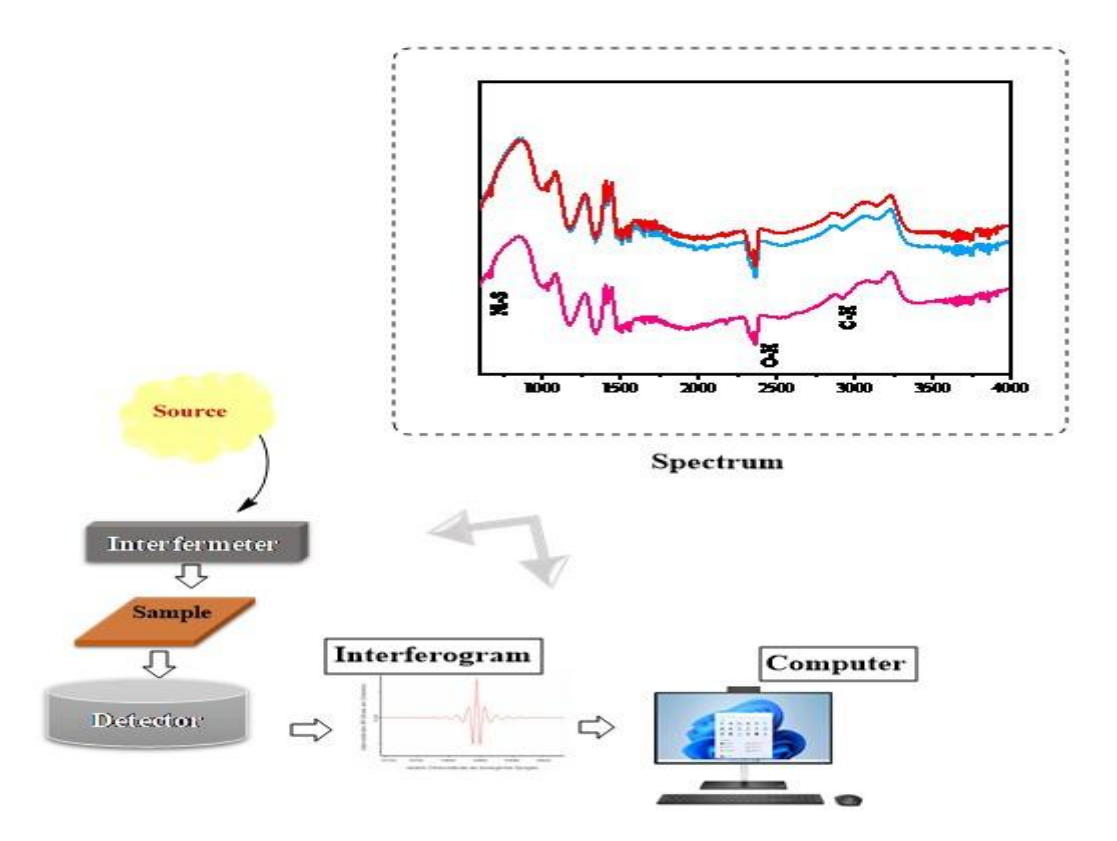


Figure (II.11): Schematic diagram of FTIR Spectrophotometer.

II. 7. Conclusion

In this chapter, we explored the experimental procedures involved in thin film deposition, focusing on spray pyrolysis techniques. We began with an introduction to thin film deposition methods, followed by an in-depth discussion of spray pyrolysis. The experimental work section detailed the preparation of solutions and thin films, ensuring precise and reproducible results. Finally, characterization methods were introduced to evaluate the structural and physical properties of the deposited films. These steps provide a comprehensive approach to understanding and optimizing thin film fabrication.

References

- [1] Perednis D, Gauckler LJ. Thin film deposition using spray pyrolysis. J Electroceramics. 2005;14(2):103–11.
- [2]Prasada Rao T, Santhosh Kumar MC. Physical properties of Ga-doped ZnO thin films by spray pyrolysis. J Alloys Compd. 2010;506:788–93.
- [3]Arthur JR. Specimen handling, preparation, and treatments in surface characterization. New York: Plenum Publishers; 1998.

- [4]Filipovic L, Selberherr S, Mutinati GC, Brunet E, Steinhauer S, Köck A, et al. Methods of simulating thin film deposition using spray pyrolysis techniques. Microelectron Eng. 2014;117:57–66.
- [5] Nie P, Xu G, Jiang J, Dou H, Wu Y, Zhang Y, et al. Aerosol-spray pyrolysis toward preparation of nanostructured materials for batteries and supercapacitors. Small Methods. 2018;2:1–24.
- [6]Pedanekar RS, Shaikh SK, Rajpure KY. Thin film photocatalysis for environmental remediation: a status review. Curr Appl Phys. 2020;20:931–52.
- [7]Youcef B. Elaboration and characterization of thin layers of zinc oxide (ZnO) deposited by ultrasonic spray for photovoltaic and optoelectronic applications [dissertation]. Biskra: University Mohamed Khider; 2019.
- [8] Madler L. Liquid-fed aerosol reactors for one-step synthesis of nano-structured particles. Chem Eng Commun. 2004;22:107–20.
- [9]Gauckler DB, AD, ARS, LJ. Spray pyrolysis of La₀ .₆ Sr₀ .₄ Co₀ .₂ Fe₀ .₈ O₃ -δ thin film cathodes. J Electroceramics. 2006;16.
- [10]Sbaihi A. Enhancement of superconducting properties of MgNiS by using oxygenannealing atmosphere [dissertation]. Biskra (DZ): University of Mohamed Khider of Biskra; 2024.
- [11]Perednis D. Thin film deposition by spray pyrolysis and the application in solid oxide fuel cells [dissertation]. Zurich: EidgenössischeTechnischeHochschule (ETH); 2003.
- [12] Vigui JC, Spitz J. Chemical vapordeposition at lowtemperatures. J Electrochem Soc
- [13] Migue, Pinto, Neves N. Al-dopedZnOceramicsputteringtargetsbased on nanocrystallinepowdersproduced by emulsiondetonationsynthesis deposition and application as a transparent conductive oxide material [dissertation]. Nova LiboaUniversity; 2015.
- [14]Srinivasulu T, Saritha K, Reddy KTR. Synthesis and characterization of FedopedZnOthin films deposited by chemical spray pyrolysis. Mod Electron Mater. 2017;3:76–85.
- [15] Cheng H, Zhai X, Ouyang J, Zheng L, Luo N, Liu J, et al. Achieving a high energystoragedensity in Ag(Nb,Ta)O₃ antiferroelectric films via nanograin engineering. J Adv Ceram. 2023;12:196–206.
- [16] Ghougali M. Elaboration and characterization of nanostructuringNiOthin films for gassensing applications [dissertation]. Biskra:University of Mohamed Khider; 2019.

- [17]Khedmi N, Ben Rabeh MK. Structural, morphological and optical properties of SnSb₂ S₄ thin films grown by vacuum evaporationmethod. Thin Solid Films .2019;669:633–40.
- [18] Anouar Y. Optimization of indium oxide thin films propertiesprepared by sol gel spin coating process for optoelectronic applications. University Mohamed Khider of Biskra, 2020.
- [19]Zaouche C, Aoun Y, Benramache S, Gahtar A. Synthesis and Characterization of DepositedNiOThin Films by Spray Pyrolysis Technique. Sci Bull Valahia Univ - Mater Mech2019;17:27–32
- [20]Benramache S, Benhaoua B. Influence of substratetemperature and Cobalt concentration on structural and optical properties of ZnOthin films prepared by Ultrasonic spray technique. Superlattices Microstruct 2012;52:807–15.
- [21]Hamedani HA. Iinvestigation of depositionparameters in ultrasonic spray pyrolysis for fabrication of solid oxide fuel cell cathode. Georgia Institute of Technology, 2008.

Chapter three:

Results and Discussion

III.1. Introduction

Nickel sulfide (NiS) is a p-type semiconductor with a low band gap of roughly 0.5 eV [3] and is one of the most significant transition metal chalcogenides due to its features as a metal-insulator and paramagnetic-antiferromagnetic phase shifting material [4]. It exhibits a variety of and stoichiometry, including NiS (a-NiS and b-NiS), NiS2, Ni3S2, Ni3S4, and Ni7S6 [5]. There are two hexagonal phases (α -NiS, P63/mmc and NiAs structure) that are stable at high temperatures (>379), as well as rhombohedral (β -NiS, R3 m, millerite) [6-8].

The aim of this research is to study a new material based on the F doped NiS thin films, which can be utilized as p-type transparent conducting oxides. This material con not studied previously in any research, the use of F with F⁻¹ to find a good transparency and free oxygen. We have studied the effect of F doping on structural, optical and electrical properties of NiS thin films.

III.2. Experimental procedure

F doped NiS solutions were prepared by dissolving (0.15 M) an amount of nickel nitrate hexahydrate $(Ni(NO_3)_2.6H_2O)$ and thiourea $(CS(NH_2)_2)$ as a source of nickel Ni and sulfur S respectively, and ammonium fluoride (NHF_4) with the ratio of F/S = 0.01 to 0.05. The mixtures were dissolved in the solvent containing equal volumes water, and then have added a some drops of HCl solution as a stabilized, the mixture solution was stirred at 50 °C for 120 min to yield a clear and transparent solution.

F doped NiS solutions were sprayed on the heated glass substrates by a spray pneumatic method which it is transform the liquid to a stream formed with uniform and fine droplets of 25 μ m average diameters. The deposition was performed at a substrate temperature of 270 °C with deposition rate was 2 mL/ min.

The obtained F doped NiS thin films have been characterized at room temperature using an X-ray diffractometer (Bruker-AXS type 8D, with $\lambda = 0.15406$ nm and 20: 20-70°). The Infra-Red Spectrometer, type (PERKINELMER Spectrum Two) was used in the frequency range of 500-4000 cm-1 to study the chemical bonding properties of the prepared films. The surface roughness of the films was analyzed using atomic force microscopy (AFM; SPI 3800 N).

III.3. Structural properties

Figure III. 1 displays the XRD patterns of fluoride-doped NiS thin films at various doping levels (0%, 1%, 3% and 5%). All samples exhibit distinct peaks at the <010>, <011>, <012>, <110>, and (022) planes, confirming their polycrystalline nature and hexagonal structure with space group P63/mmc, in accordance with ICSD card No. 98-060-2488. No other fluoride-related phases are detected; also we have not observed any related phase of NiO in the XRD spectra's.

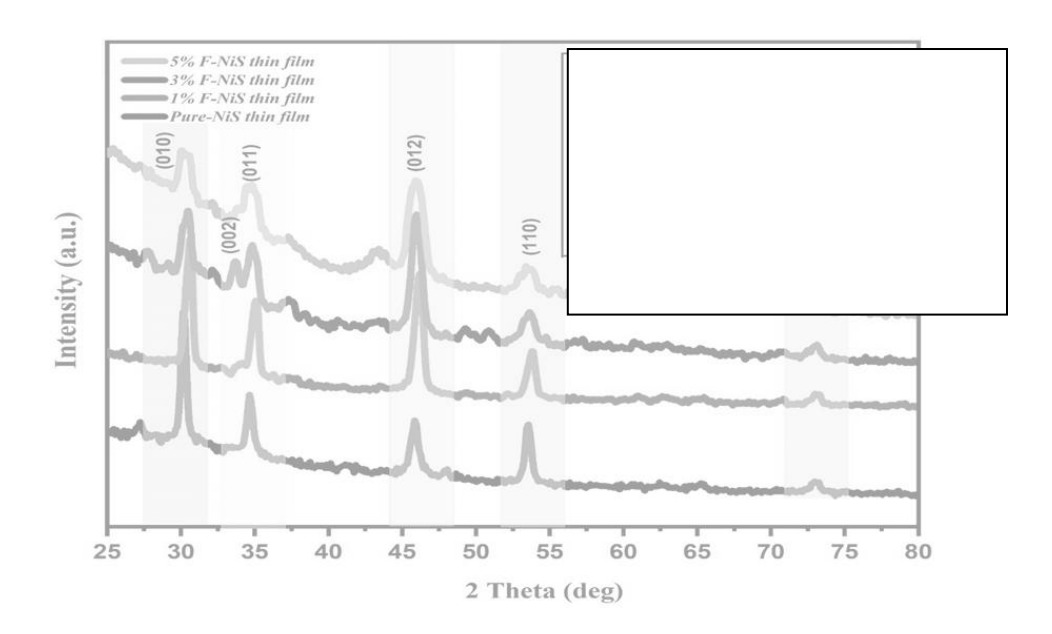


Figure III.1: X-Ray diffraction spectra of F doped NiS thin films elaborated at 270°C with various F doping ratio (at.%). The inset graph shows diffraction angle and intensity peaks of the ICSD card No. 98-060-2488.

The effects of F doping on crystal structure and favored orientations were studied by characterizing all sprayed F doped NiS thin films using the XRD technique. **Figure III.2** shows the effect of F doping on the shifting of specified angle to form the plane (012). Fluorine (F) doping in materials like NiS can cause shifts in the diffraction peaks of X-ray diffraction (XRD) patterns, particularly affecting the (012) plane (see **Figure III.2b**). Specifically, F doping can lead to a increase in the intensity and a shift towards higher angles of the (012) peak. However, the **Figure III.2a** whiles the (010), (011) and (110) peaks might show decreased intensity after 1at% with shift towards lower angles. These changes are attributed to the F ion's smaller ionic radius compared to oxygen, which can induce lattice deformation.

The crystallite size D_{hkl} of the films was calculated for the four higher plane using Scherrer's formula [9,10]:

$$D_{hkl} = \frac{k\lambda}{\beta\cos\theta} \tag{III.1}$$

The Micro-Strain ε_{hkl} was calculated using Stokes-Wilson relation [11]:

$$\varepsilon_{hkl} = \frac{\beta}{4\tan\theta} \tag{III.2}$$

The interplanar spacing d_{hkl} is calculated by Bragg's law [12]:

$$2d_{hkl}\sin\theta = n\lambda \tag{III.3}$$

The lattice parameters a and c of F doped NiS hexagonal structure can be determined by using the following formula [13]:

$$d_{hkl} = \frac{a}{\sqrt{\frac{4}{3}(h^2 + k^2 + hk) + l^2 \frac{a^2}{c^2}}}$$
(III.4)

where : β (rad) is full width at half maximum FWHM, λ is the wavelength of X-ray ($\lambda = 0.15406$ nm), k is a constant (k = 0.9).

Table III.1 show the crystal structure corresponding to each<hkl> plane, which are presented the diffraction angle of each <hkl> plane corresponded to the ICSD card No. 98-060-2488 (see **Table III.2**). The variation of crystallite size D_{hkl} of (010), (011), (012) and (110) planes are presented in **Table III.3**, we notice that the sizes of the crystallites oriented along the (012) crystallographic plane decrease with doping ratio, these evolutions indicate that F doping deteriorates the crystallinity of NiS thin films. However, the micro-Strain ε_{hkl} are also calculated from (010), (011), (012) and (110) planes to be used for confirming the effect of F doping (see **Table III.4**). We observed that the micro-strain increased with increasing of f doping from 0 to 5 at% for each plane, we noticed that there is changes are attributed to the F ion's smaller ionic radius compared to oxygen, which can induce lattice deformation.

Table III.1: The crystal structure corresponding to each<hkl> plane.

2 Theta	<hkl></hkl>	Structure Crystal		References	
			Structure		
30.104	<010>	NiS	Hexagonal	98-060-2488	
33.863	<002>	NiS	Hexagonal	98-060-2488	
34.556	<011>	NiS	Hexagonal	98-060-2488	
45.865	<012>	NiS	Hexagonal	98-060-2488	
53.278	<110>	NiS	Hexagonal	98-060-2488	
72.886	<022>	NiS	Hexagonal	98-060-2488	

Table III.2: The the diffraction angle corresponding to each <hkl>plane.

Sample	2 Theta			
	(010)	(011)	(012)	(110)
Pure NiS thin Film	31.251	31.643	44.775	55.710
1% F: NiS thin Film	31.717	34.208	45.262	54.862
3% F : NiS thin Film	31.527	33.957	44.899	54.742
5% F : NiS thin Film	31.536	34.054	45.103	54.877

Table III.3: The Crystallite size values for each <hkl>plane of FxNiS1-x films.

Sample	Pure NiS thin	1% F: NiS thin	3% F: NiS thin	5% F: NiS thin	
D (hkl)	Film	Film	Film	Film	
<010>	20.33	17.17	15.26	10.93	
<011>	19.64	16.64	12.92	9.60	
<012>	14.85	14.53	12.31	8.37	
<110>	19.01	15.32	11.51	9.95	

Table III.4: The Micro-Strain values for each <hkl>plane of FxNiS1-x films.

Sample	Pure NiS thin	1% F: NiS thin	3% F: NiS thin	5% F: NiS thin
$\epsilon_{(hkl)}.10^{-3}$	Film	Film	Film	Film
<010>	6.55	7.63	8.63	12.05
<011>	5.92	6.89	8.94	11.99
<012>	5.99	6.10	7.22	10.58
<110>	4.05	5.00	6.67	7.71

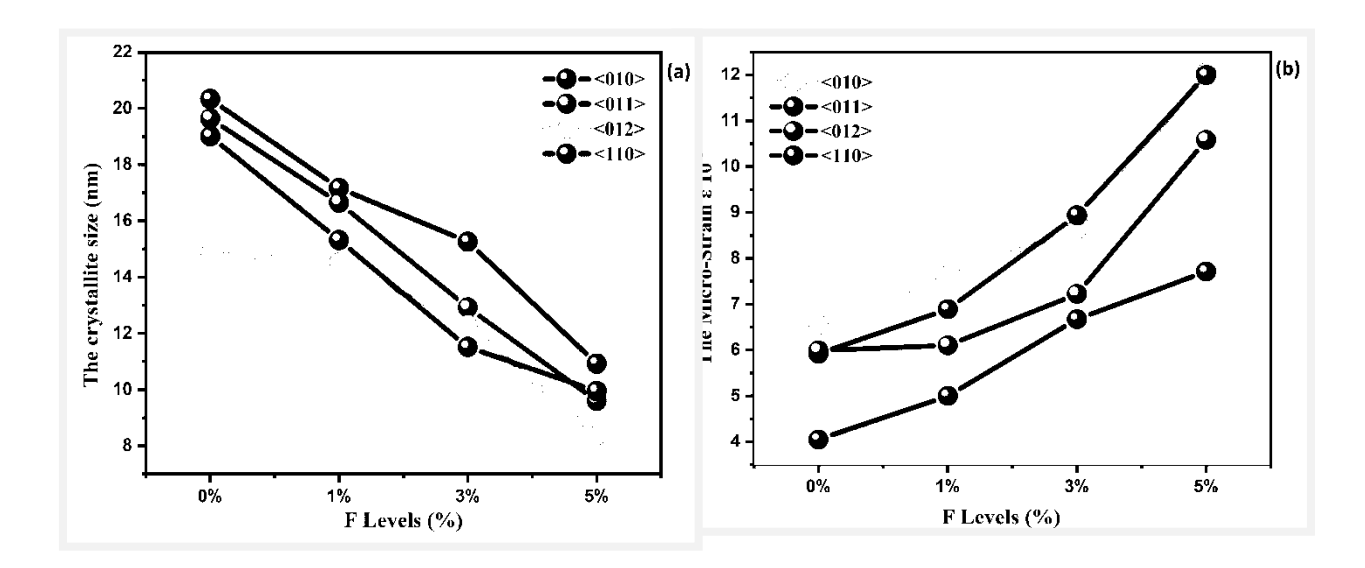


Figure III.3: a): Variation of crystallite size b): Variation of micro-strain values of F doped

NiS thin film.

Figure III.3a shows the crystallite size of four diffraction peaks (010), (011), (012) and (110). The crystallite size was varied between 8 and 21 nm, and these results indicate that the F doped NiS thin films exhibit a polycrystalline nature. The crystallite size was decreased with increasing of F doping from 0 to 5 at%; this indicates that the atomic radius of F lower than the O; this is attributed to the improvement of the crystalline structure of F doped NiS thin films. However, we have observed that the crystallite size of (010) plane higher than others plans due to the high peak intensity; this is attributable to an decrease in the FWHM.

Figure III.3b We observed that the micro-strain increased with increasing of f doping from 0 to 5 at% for each plane, we noticed that there is changes are attributed to the F ion's smaller ionic radius compared to oxygen, which can induce lattice deformation.

III.5. FTIR Spectroscopy results

The F doped NiS thin films samples were studied by FT-IR spectroscopy (Fourier Transform Infrared). The specters of F doped NiS samples measured in the range of 500-4000 cm-1 using a spectrophotometer infrared type of (PERKINELMER Spectrum Two), it shown

in **Figure III.4**. As shown in **Figure III.4**, for all samples, the characteristic peaks are 2939, 2348, 1037 and 624 cm⁻¹ correspond to the Ni-S, C-O, C-S and Ni-S bonds, respectively [14-17].

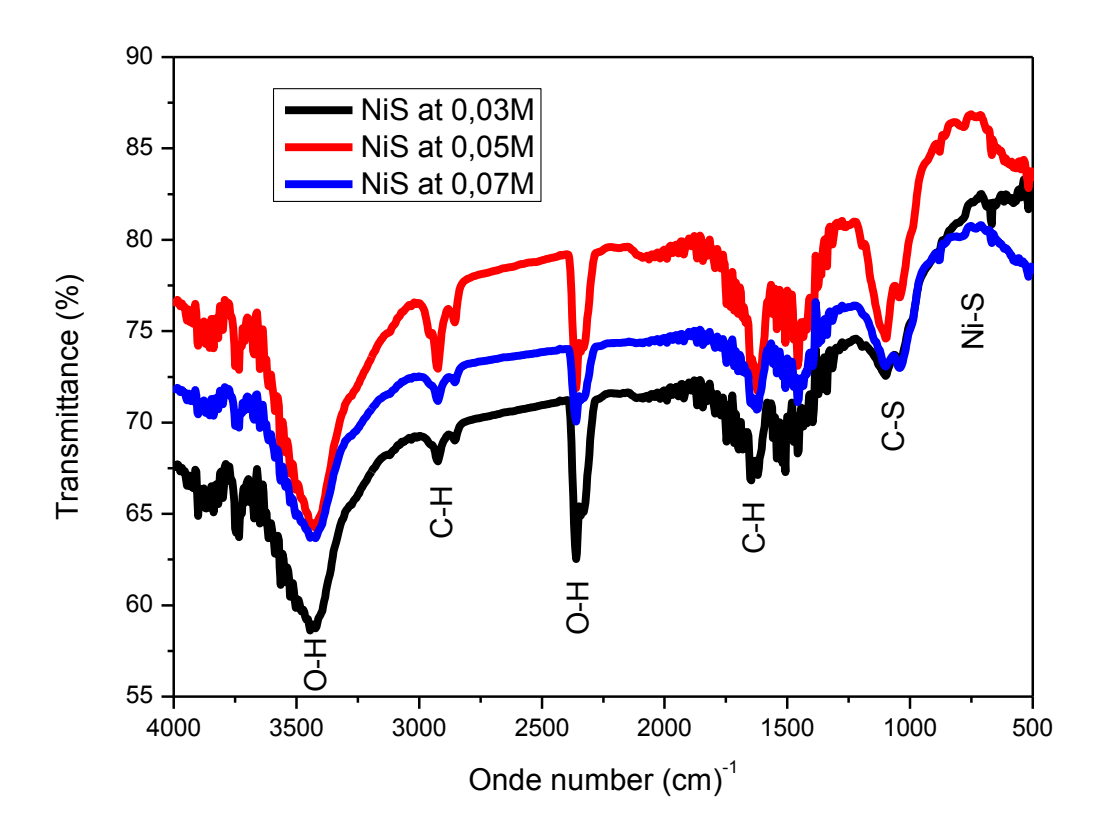


Figure III.4: FTIR spectra of F doped NiS thin film prepared with various fluoride doping.

III.6. Electrical properties

The four-point probe is required to measure the sheet resistance of F doped NiS films. Since negligible contact and spreading resistance are associated with the voltage probes, the sheet resistance (R_{Sh}) can be estimated, when the film thickness less than the spacing between the probes, using the following relation [11,12]:

$$R_{\rm sh} = \frac{\pi}{\ln(2)} * \frac{V}{I} \tag{III.5}$$

where *I* is the applied current and *V* is the measurement voltage.

Table III.5 The electrical resistance Cu and F co-doped ZnO thin films

F doped NiS thin films	0%	1 at%	3 at%	5 at%
$R_{\mathrm{sh}}\left(\Omega\right)$	5.304	1.052	4.115	10.219

The electrical measurements were conducted only on the film prepared with 0.05 M. It seems that the electrical current in the films perpared with the two other concentration was very high and exeeds the limit of the instrument used in our study. Therfore, no data were recorded for these two samples. Fig. IV.9 depicts the temperature dependence of the ac-conductivity (σ_{ac}). As can be seen, σ_{ac} increases with the increase in the temperature from 1.97×10^3 S/cm (at 310 K) to 2.24×10^3 S/cm (at 378 K). This behavior is typical in semiconducting materials according to Arrhenius law. The ac-conductivity is expressed by:

$$\sigma = \sigma_0 Exp\left(-\frac{E_a}{kT}\right)....(IV.15)$$

where k is the Boltzmann constant and T the absolute temperature. The linear fit of the curve of log (σ_{ac}) vs. 1000/T, yields an activation energy (E_a) of 26.7 meV.

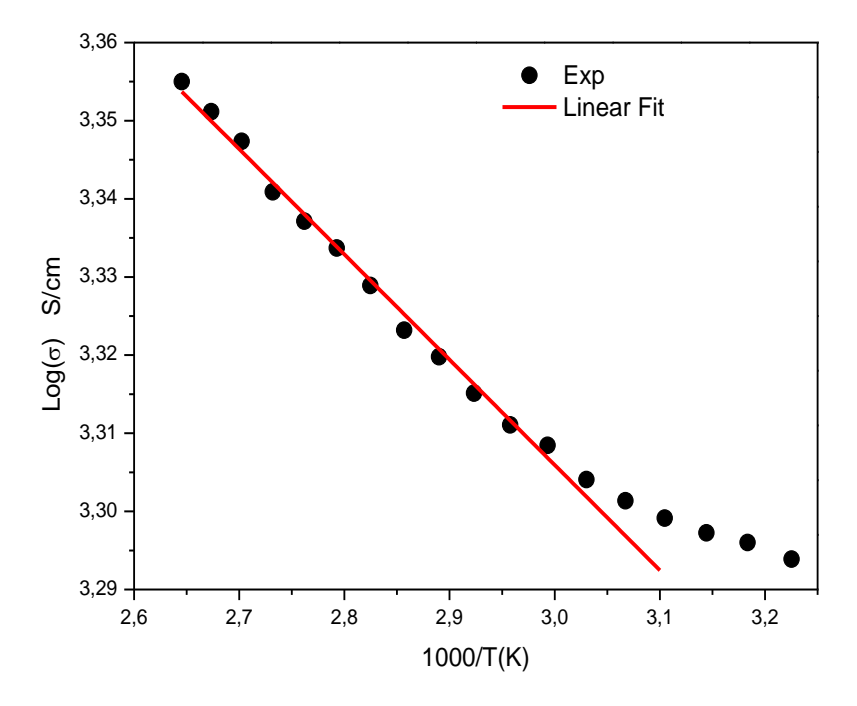


Figure III.7 Temperature dependence of the ac-conductivity of the NiS film prepared with 0.05 M.

III.7. Conclusions

In conclusion, the F doped NiS thin films were successfully deposited on glass substrate by spray pneumatic method. F doped NiS solutions were prepared by dissolving (0.15 M) an amount of nickel nitrate hexahydrate (Ni(NO₃)₂.6H₂O) and thiourea (CS(NH₂)₂) as a source of nickel Ni and sulfur S respectively, and ammonium fluoride (NHF₄) with the ratio of F/S = 0.01 to 0.05. The effect of F doping on structural, optical, morphologically and electrical properties were investigated. The prepared F doped NiS thin films have a polycrystalline nature with a hexagonal structure, the (012) diffraction peak is the preferred orientation. The FTIR analysis showed the characteristic vibration bands of NiS. The AFM analysis revealed that nanometer sized spherical grains cover the entire surface of the films prepared. The minimum sheet resistance was found for the thin film prepared with 1 at% F

References

- [1] J. Younus, W. Shahzad, B. Ismail, T. Fazal, M. Shah, Sh. Iqbal, A. H. Jawhari, N. S. Awwadf, H. A. Ibrahiumg, Engineering the optical properties of nickel sulphide thin films by zinc integration for photovoltaic applications, RSC Advances, 13 (2023) 27415.
- [2] A. Gahtar, C. Zaouche, A. Ammari, L. Dahbi, Growth and characterization of bimetallic (Ni,Co) sulfide thin films deposited by spray pyrolysis, ChalcogenideLetters, 20 (2023) 377-385.
- [3] V. Kumar, D.K. Sharma, K. Sharma, D.K. Dwivedi, Investigation on physical properties of polycrystalline nickel sulphide films grown by simple & economical screen-printing method, Optik 156 (2018) 43-48.
- [4] X. Shen, J. Sun, G. Wang, J. Park, K. Chen, A facile single-source approach to urchin-like NiS nanostructures, Materials Research Bulletin 45 (2010) 766-771.
- [5] Ch. Buchmaier, M. Glanzer, A. Torvisco, P. Poelt, K. Wewerka, B. Kunert, K. Gatterer, G. Trimmel, T. Rath, Nickel sulfide thin films and nanocrystals synthesized from nickel xanthate precursors, J Mater Sci 52 (2017) 10898-10914.
- [6] S. Mehta, K. S. Samra, Metal-sulfide based nano-composites and their electrochemical performance: A Review, Journal of Physics: Conference Series 2267 (2022) 012004.
- [7] G. Kullerud, R. A.Yund, The Ni-S system and related minerals. J Petrol, 3(1962) 126-175.
- [8] R. Boughalmi, R. Rahmani, A. Boukhachem, B. Amrani, K.D. Khodja, M. Amlouk, Metallic behavior of NiS thin film under the structural, optical electrical and ab initio investigation frameworks, Mater. Chem. Phys, 63 (1) (2015) 99-106.

- [9] A. Gahtar, S. Benramache, C. Zaouche, A. Boukacham, A. Sayah, Effect of temperature on the properties of nickel sulfide films performed by spray pyrolysis technique, Advances in materials science, 20 (2020) 36-51.
- [10] S. Benramache, B. Benhaoua, Influence of substrate temperature and Cobalt concentration on structural and optical properties of ZnO thin films prepared by Ultrasonic spray technique, Superlattices Microstruct, 52 (2012) 807-815.
- [11] S. Benramache, B. Benhaoua, H. Guezzoun, Study the Effect of Cu Doping on Optical and Structural Properties of NiO Thin Films, Annals of West University of Timisoara-Physics 62 (2020) 15-22.
- [12] S.C. Bulakhe, R.J. Deokate, Electrochemically prepared Fe: NiO thin film catalysis for oxygen evolution reaction. J Mater Sci: Mater Electron 33, 18180–18186 (2022).
- [13] M. Sathya, G. Selvan, M. Karunakaran et al. Synthesis and characterization of cadmium doped on ZnO thin films prepared by SILAR method for photocatalytic degradation properties of MB under UV irradiation. Eur. Phys. J. Plus 138 (2023) 67.
- [14] A. Gahtar, S. Benramache, A. Ammari, A. Boukhachem, A. Ziouche, Effect of molar concentration on the physical properties of NiS thin film prepared by spray pyrolysis method for supercapacitors, Inorganic and Nano-Metal Chemistry, (2021).
- [15] R. S. Ali, H. S. Rasheed, N. D. Abdulameer, N. F. Habubi, S. S. Chiad, Physical properties of Mg doped ZnS thin films via spray pyrolysis, chalcogenide letters, 20 (2023) 187-196.
- [16] Ghezelbash, A.; Sigman, M. B.; Korgel, B. A. Solventless, Synthesis of Nickel Sulfide Nanorods and Triangular, Nanoprisms. Nano Lett. 2004, 4, 537–542.
- [17] Karthikeyan, R.; Thangaraju, D.; Prakash, N.; Hayakawa, Y. Single-Step Synthesis and Catalytic Activity of Structure-Controlled Nickel Sulfide Nanoparticles. CrystEngComm 2015, .5439–5431,17

Chapter three:

Results and Discussion

General Conclusion

General Conclusion

General Conclusion

The aim of this research is to study a new material based on the F doped NiS thin films, which can be utilized as p-type transparent conducting oxides. This material con not studied previously in any research, the use of F with F⁻¹ to find a good transparency and free oxygen. We have prepared an alloy of F doped NiS at various F doping concentrations for study the effect of F doping on structural, optical, morphologically and electrical properties. These films are applied using a single technique: spray pyrolysis.

- ✓ F doped NiS solutions were prepared by dissolving (0.15 M) an amount of nickel nitrate hexahydrate (Ni(NO₃)₂.6H₂O) and thiourea (CS(NH₂)₂) as a source of nickel Ni and sulfur S respectively, and ammonium fluoride (NHF₄) with the ratio of F/S = 0.01 to 0.05.
- ✓ The F doped NiS thin films were successfully deposited on glass substrate by spray pneumatic method.
- ✓ The effect of F doping on structural, optical, morphologically and electrical properties of NiS thin films were investigated.
- ✓ The prepared F doped NiS thin films have a polycrystalline nature with a hexagonal structure, the (012) diffraction peak is the preferred orientation.
- ✓ The minimum value of crystallite size (D=9.95nm) was observed for 5 at% F doping.
- ✓ The maximum value of micro-strain ($e=12.05*10^{-3}$) was observed for 5 at% F doping.
- ✓ The FTIR analysis showed the characteristic vibration bands of NiS.
- ✓ The AFM analysis revealed that nanometer sized spherical grains cover the entire surface of the films prepared.
- ✓ The minimum sheet resistance was found for the thin film prepared with 1 at% F.